Norwegian Meteorological Institute
met.no
met.no report
no. 1/2012
Meteorology

Assimilation of radar reflectivity data in HARMONIE

Martin S. Grønsleth and Roger Randriamampianina

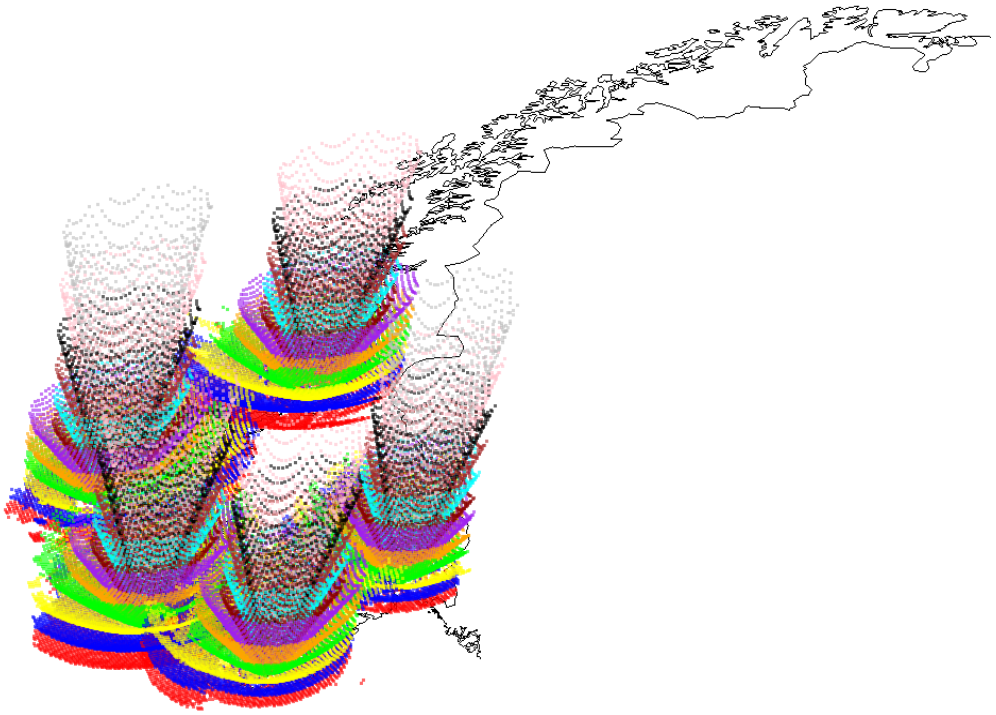

Figure 1: Radar reflectivity observations available for the HARMONIE/AROME assimilation system before screening 2011-09-03 06:00 UTC from the five southernmost radars in Norway. Different colors for each elevation.

Norwegian Meteorological Institute
met.no

report

Title Assimilation of radar reflectivity data in HARMONIE	**Date** 2012-01-30
Section Numerical Weather Prediction (NWP)	**Report no.** no. 1/2012
Author(s) Martin S. Grønsleth and Roger Randriamampianina	**Classification** ◉ Free ○ Restricted
	ISSN 1503-8025
	e-ISSN 1503-8025
Client(s) Energi Norge (EBL), The Research Council of Norway	**Client's reference** NFR ES439901/193048

Abstract

The work described in this report has been conducted within the Energi Norge (EBL) project "Utnyttelse av værradardata i værvarslings- og tilsigsmodeller", lead by SINTEF Energy with funding from Energi Norge members, The Research Council of Norway and own funding from met.no. This report covers the achievements in subproject 2, mainly subproject 2.2 "Assimilasjon av radarreflektivitet i full ikke-hydrostatisk atmosfæremodell" ("Assimilation of radar reflectivity in a fully non-hydrostatic atmospheric weather model").

Introductory tests of the weather model and assimilation system are presented, using the HARMONIE model and the AROME physics package. The treatment of the converted Norwegian radar observations in the system is reported. This is followed by a case study of the impact of radar reflectivity data. The method used for radar data assimilation was adopted from Météo-France.

The report demonstrates that a technically working pre-operational system for assimilating radar data has been set up. Although preliminary, verification scores of a two weeks impact study show positive impact when including radar reflectivity in the analysis system. And, yet unresolved issues are discussed.

Keywords

Assimilation, radar data, reflectivity, radial wind, doppler wind, NWP, Harmonie, Arome, 3DVAR

Disiplinary signature **Responsible signature**

Abstract

The work described in this report has been conducted within the Energi Norge (EBL) project "Utnyttelse av værradardata i værvarslings- og tilsigsmodeller", lead by SINTEF Energy with funding from Energi Norge members, The Research Council of Norway (NFR ES439901/193048) and own funding from met.no. This report covers the achievements in subproject 2, mainly subproject 2.2 "Assimilasjon av radarreflektivitet i full ikke-hydrostatisk atmosfæremodell" ("Assimilation of radar reflectivity in a fully non-hydrostatic atmospheric weather model").

Introductory tests of the weather model and assimilation system are presented, using the HARMONIE model and the AROME physics package. The treatment of the converted Norwegian radar observations in the system is reported. This is followed by a case study of the impact of radar reflectivity data. The method used for radar data assimilation was adopted from Météo-France.

The report demonstrates that a technically working pre-operational system for assimilating radar data has been set up. Although preliminary, verification scores of a two weeks impact study show positive impact when including radar reflectivity in the analysis system. And, yet unresolved issues are discussed.

Acknowledgements

The authors want to thank Energi Norge and The Research Council of Norway, RCN (NFR/193048) for the funding of this project. SINTEF is leading the project, and we appreciate the good collaboration with them. The data simulations have been run at the supercomputer facility at ECMWF using the national quota, and in addition the special project SPNOHARM. Météo-France is acknowledged for providing reflectivity routines in HARMONIE and BUFR documentation – a special thanks goes to Thibaut Montmerle and Eric Wattrelot. Nils Gustafsson is acknowledged for providing the background error statistics, and for giving valuable feedback.

The encouragement, support and help from the colleagues at the R&D department is greatly appreciated. We would also like to thank the colleagues at the Metklim department for fruitful discussions, and would like to express a special thanks to Christoffer A. Elo and Morten Salomonsen for the good collaboration on data exchange.

Parts of this report was carried out at The Hungarian Meteorological Service (OMSZ), and the visiting author was given a warm welcome and hospitality during the stay.

Support from the HIRLAM community, the ALADIN community and the ECMWF staff has also been of great importance during the project.

Contents

List of Figures

List of Tables

Chapter 1

Introduction

Thanks to the fast development in computing technology, the implementation of a very high resolution numerical weather prediction (NWP) model becomes affordable. At met.no the HARMONIE limited area model (LAM) in its AROME version, with horizontal grid mesh of 2.5 km, is being implemented. The accuracy of the NWP forecast depends in part on the quality of the initial conditions. The initial conditions for a LAM can be constructed (downscaled) from a global or an other LAM analysis or forecast. The potentially best way for creating the initial conditions for NWP models is, however, reached by involving observations through data assimilation. It is expected that mesoscale (high resolution) models require high resolution observations. Depending on the applied assimilation technique the temporal resolution of the observations can also be crucial. Since ground based weather radars provide frequent updates (every ∼15 minutes) of three-dimensional observations at very high resolution (∼1 km), these observations are of great interest for improving the initial conditions for a mesoscale model.

Observations from ground based weather radars are currently used for providing realtime weather conditions to the public and to assist meteorologists and scientists. These observations are presented at *e.g.* `http://yr.no/radar/`. There are currently eight operational weather radars in Norway. The radar observations are, however, not yet used in the Norwegian NWP system.

Radar observations can be categorized in two main types; *reflectivity* and *wind*. This work aims at providing radar reflectivity data to the next generation NWP system, HARMONIE, using the 3DVAR (three-dimensional variational) assimilation technique. The use of the radial wind data from the radars is considered in another sub-project.

There are several ways to assimilate radar reflectivity observations in NWP models. The main approaches in use are nudging, variational analysis and ensemble Kalman filtering. Reflectivity observations requires a complicated observation operator including moist physics. A nice overview of the different approaches on the use of radar observations can be found in [1].

Chapter 2 describes the methods used: Model setup, radar data handling, and some limitations in the setup. Chapter 3 shows the result of several test experiments: Single observation experiments, single profile experiments, evaluation of the radar simulator, a case and impact studies. Concluding remarks are presented in Chapter 4.

Chapter 2

Method and data

Weather radars belong to active remote sensing devices, which means that they scan the atmosphere by sending out and detecting parts of the back-scattered electromagnetic pulses. The electromagnetic frequency is tuned so that the pulses are reflected by precipitating particles, such as rain, snow, graupel, cloud ice, etc. Since the radar scans its surroundings at different elevations, it collects information from the detectable reflectivity at different distances from the radar site. By scanning all azimuth angles, and several elevations, we get a dataset of the reflectivity of the volume around the radar. Typically, the radial range is around 240 km for reflectivity. The altitude can reach 10–15 km, and the resolution is typically given by bin sizes equal or less than 1 km. Reflectivity is measured in units of dBZ; decibel Z. Details on how weather radars function can be found in *e.g.* [2].

The relationship between the reflectivity measurements and the model control variables is very complex. Therefore, the existing data assimilation techniques cannot be used directly to assimilate the radar reflectivity data. So, alternative approaches are needed. We follow a method developed by Météo-France [3, 4, 5], which consists of combining 1D Bayesian and 3D-variational assimilation schemes, where reflectivity data is assimilated as unidimensional (1D) humidity retrievals into the three-dimensional (3DVAR) assimilation system.

2.1 HARMONIE/AROME

The operational NWP system at met.no is currently HIRLAM[1], which is a hydrostatic model that treats convection implicitly. Non-hydrostatic quasi-convection resolving models can potentially give a better description of the dynamical processes on the fine scale. This is often of great interest for the users. HARMONIE/AROME is developed with this goal, and will be the successor of HIRLAM. However, adaptation to the Norwegian climate and topography is needed, both for radar observations [6, 7] and for the model itself, in addition to technical adjustments for running the model on local HPC facilities. The HARMONIE assimilation and forecast system currently runs in experimental mode at met.no. Its non-hydrostatic version is based on the AROME meso-scale model [8]. The assimilation system includes a surface Optimal Interpolation scheme to update soil moisture content and skin temperature fields, and an upper-air spectral three-dimensional variational (3DVAR) data assimilation system to analyze wind, temperature, specific humidity and surface pressure fields. It supports conventional observations from ground- and sea-based stations (SYNOP and SHIP), wind profilers (PILOT), radiosondes (TEMP), aircraft reports (AIREP), oceanographic buoys (DRIBU), atmospheric motion vectors (AMV). It also supports assimilation of microwave radiances from AMSU-A, AMSU-B (Advanced Microwave Sounding Unit) and MHS (Microwave Humidity Sounder) from the NOAA (National Oceanic and Atmospheric Administration) series and the MetOp polar-orbiting satellites, as well as the Infrared Atmospheric Sounding Interferometer (IASI). The background-error covariances are calculated from ensemble global perturbed analyses [9] downscaled to the regional domain and projected to a 6-hour forecast [10]. The balances are purely statistical, and estimated through multi-variate linear regression [11].

[1] The community developing and using the HIRLAM and HARMONIE NWP systems, also goes by the name HIRLAM. The HIRLAM consortium consists of the meteorological institutes DMI, EMHI, FMI, VI, Met Eireann, KNMI, AEMET, SMHI, LHMS and met.no, and is also collaborating with members of the ALADIN consortium, which includes Météo-France.

2.2 Radar data assimilation

It is essential that the NWP model starts out from an initial state that is as close as possible to the corresponding true atmospheric state in order to get a good quality of forecasts. The process of objectively adapting the model state to observations in a statistically optimal way, is called *assimilation*. It takes into account both the model and the observation errors.

The information contained in the reflectivity images retrieved from the radars, is of very high spatial resolution compared to conventional observations. But the NWP model cannot use the volume data directly, since reflectivity is not a model parameter. Instead, the reflectivity needs to be converted to a quantity that can be assimilated into the system, and in turn re-initialize the model control variables. In AROME, the physics package used by HARMONIE in this work, the model variables are temperature, pressure, wind (three components), specific humidity (*i.e.* water vapor), turbulent kinetic energy, cloud fraction, and five condensed water species; three of them are precipitating (rain, snow, graupel (*i.e.* ice water mixed particles)), and two are virtually non-precipitating (cloud liquid water, cloud ice) [12]. In addition, several two-dimensional variables are computed in the surface layer and the soil. Reflectivity is assimilated as humidity profiles.

2.3 Assimilation of radar data through pseudo-observations

It is difficult to assimilate reflectivity directly into the model variables. Therefore, we have made the choice, although reflectivity directly depends on the hydrometeor content of the air, to not include those hydrometeor contents in the 3DVAR control variables. Moreover, initialization of those species is expected to have less significant impact on forecasts [3].

Variables such as humidity and temperature are expected to have great impact. Therefore, a 1D retrieval of humidity columns from reflectivity columns is performed. The retrieved humidity columns are then provided as pseudo-observations to the 3DVAR assimilation system.

A 1D Bayesian approach is used in the retrieval, as opposed to a full 1DVAR, which would require the tangent-linear and adjoint of the physical parameterizations. Because of the very non-linearity of the reflectivity forward operator, the latter could lead to convergence problems.

In the 1D Bayesian scheme, the observed reflectivity is compared with the model's first guess. This comparison requires the model parameters to be translated into simulated reflectivity. This is done by the forward operator, $H(x)$, which in the case of reflectivity is highly non-linear.

More on the 1D Bayesian method can be found in [5, 3] and on the radar simulator in [13]. One of the benefits of the method is that it is computationally feasible, while the main drawbacks are that if *e.g.* convective cells are observed at locations where the model background have no such cells in near vicinity, the method will not be able to create representative pseudo-observations of humidity. This is compensated by a "humidity adjustment", raising the value of relative humidity to 100 %, for more details see [5].

2.3.1 Pre-processing and quality flags

In addition to the quality control done by the radar hardware/software on site, a lot of effort is put into refining the radar products further. This is done by *e.g.* adding quality flags for each pixel of data, based on various techniques. At met.no, the versatile and modular PRORAD framework at the Remote Sensing division, takes care of this [7]. Quality control algorithms implemented in the PRORAD framework within this project are described in [6, 14].

Currently, PRORAD support quality flags for sea-clutter, ground-clutter and other-clutter (*i.e.* boats etc.), classification flags, and indicators to whether a pixel contains an observation or not. The full list of quality flags is shown in Table 2.1.

PRORAD stores reflectivity data and quality flags in an XML format called PRORAD XML. These files constitute the best achievable refined product from the Norwegian radar network. But before it can be used in the HARMONIE system, it must be converted to a format recognized by the observation processing module (BATOR). The development of such a conversion program was initiated in sub-project 2.1, and is

Table 2.1: Quality flags in PRORAD

Flag	Meaning
`is_nodata`	Pixel contains no data (*e.g.* out of range)
`is_lowele`	Used for PCAPPI product
`is_highele`	Used for PCAPPI product
`is_blocked`	Pixel is blocked (by *e.g.* mountain)
`block_percent`	Percentage of blockade
`is_seaclutter`	Pixel is polluted by sea-clutter
`is_groundclutter`	Pixel is polluted by ground-clutter
`is_otherclutter`	Pixel is polluted by other clutter
`clutter_probability`	Probability of given clutter type

called CONRAD [15, 16, 17]. It has been further developed and improved within sub-project 2.2 in order to comply with changes in both ends of the data chain.

The data flow is illustrated in Figure 2.1. When the observations are in the ODB (Observational DataBase), they are ready for use by the assimilation system.

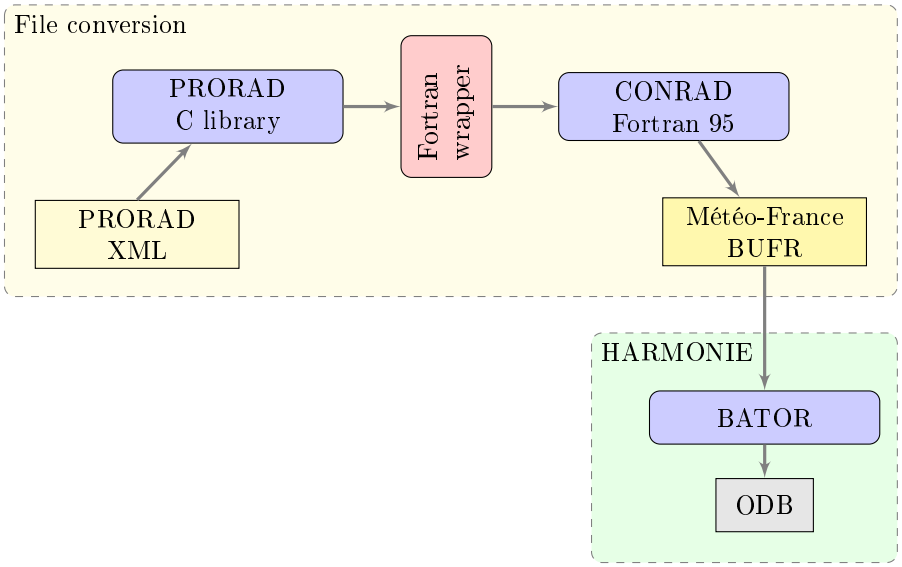

Figure 2.1: A schematic overview of the data flow of the Norwegian radar data into the NWP system.

Chapter 3 describes how the accuracy of the preprocessing and the analysis systems was progressively checked and tested.

2.3.2 Assumptions and approximations

There are several assumptions and approximations in the treatment of the radar data. Already at the radar site, the radar software makes a number of assumptions about the earth curvature, the weather dependent refraction of the radar beam (ducting), and the actual strength of the echo, to mention a few.

The shape of the earth is assumed to be spherical, although this is not the case. Also, since the electromagnetic pulse is propagating through air layers of different density, the beam will be subject to refraction. To compensate for this, an effective radius of 4/3 of the equatorial radius of the earth is used.

Furthermore, data interpolation is needed in the process of converting the data between the different file formats. The native PRORAD XML format is polar volumetric data, while the BUFR file reader in HARMONIE, named "BATOR", demands[2] cartesian PPIs with pixel dimension 512×512.

[2]This is subject to change in the future. Support for polar data in BATOR is in the making.

On the NWP side, certain approximations are taken when the volume of reflectivities is converted into columns of humidity pseudo-observations: Although the volume is represented as consecutive slices of PPIs, they do not map pixel-by-pixel vertically, due to geometrical reasons. This effect is strengthen by the earth curvature. In BATOR it is, however, taken as an approximation that the latitude/longitude position of pixels in the first elevation is valid also for pixels in higher elevations with the same row/column position in the dataset. In principle, this means that the far out columns of humidity will tilt towards the radar site, while they are used as true vertical profiles in the assimilation. The mismatch will be biggest farthest away from the radar, for the highest elevations.

Another limitation of the current setup, is that the forward operator, $H_Z(x)$, calculating simulated reflectivity, does not take into account the blockage map for the Norwegian radars. It is therefore assuming clear sight for all radars, which is not the case. This can lead to problems with simulated observations in partially blocked spots.

Chapter 3

Results

Radar reflectivity data is assimilated as vertical profiles of humidity, and it is therefore of great importance to know how the system reacts on injections of such (pseudo-)observations. How does the background error covariance influence the various other control variables, are the increments realistic, etc. This is covered in Section 3.2. In Section 3.3 and 3.4 reflectivity observations are considered. The radar reflectivity operator (radar simulator) is investigated in Section 3.5 using full volumetric input data. A case study (with verification data) is given in Section 3.6, and concluding remarks can be found in Chapter 4.

3.1 Image orientation

A small test image was prepared in order to verify that the orientation of the radar picture is not altered in the conversion chain. Correspondence is shown in Figure 3.1. The raw data image was artificially created, saved as a PRORAD XML, converted by CONRAD to the Météo-France BUFR format, sent through BATOR and ended in the ODB ready for assimilation by HARMONIE. The data was thinned in the process, so only every fifth reflectivity value is available in the ODB. Also, there is a cut-off in BATOR, accepting only data up to a radial distance of 160 km. In Figure 3.1b and 3.1c, data as retrieved from ODB is presented, showing that the structure and orientation of the raw data (Figure 3.1a) is kept in the process.

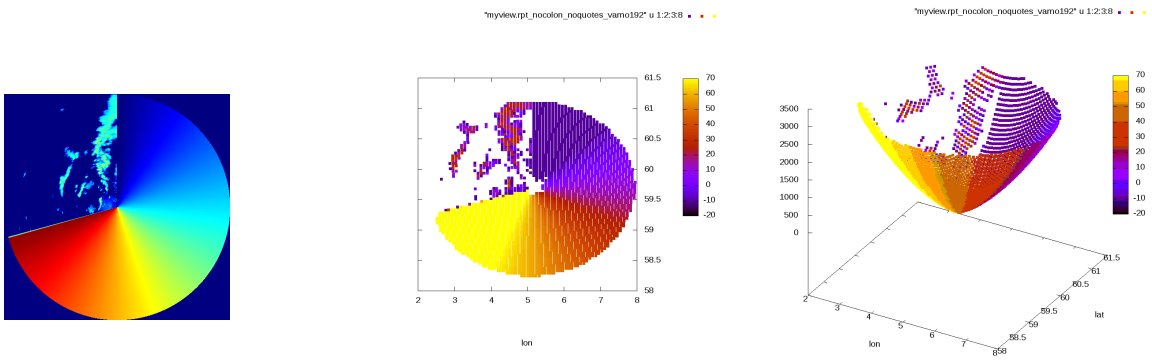

(a) Pixel values in raw data (radial range ∼240 km)

(b) dBZ values retrieved from ODB, seen from above (radial range ∼160 km)

(c) dBZ values retrieved from ODB, 3D view (radial range ∼160 km)

Figure 3.1: Verification of picture orientation, comparing PPIs (Plan Position Indicator) of **(a)** raw input data and **(b,c)** as obtained from the ODB (Observational database). Note that the color maps do not correspond, and that the radial range is different in **(a)** and **(b,c)**.

3.2 Single humidity profile observation experiment

In this section, the results of a single humidity profile experiments is reported.

A single humidity profile located at lat 58.87000 N, lon 5.67000 E (encoded as radiosonde data from WMO ID 01415, valid at 2010-09-09 hour 12) has been assimilated to investigate the model response. The experiment was run with HARMONIE 36h1.1, using AROME with 2.5 km resolution over an area covering a large part of south of Norway (`NORWAY_SOUTH_BIG`). The location is shown in Figure 3.2.

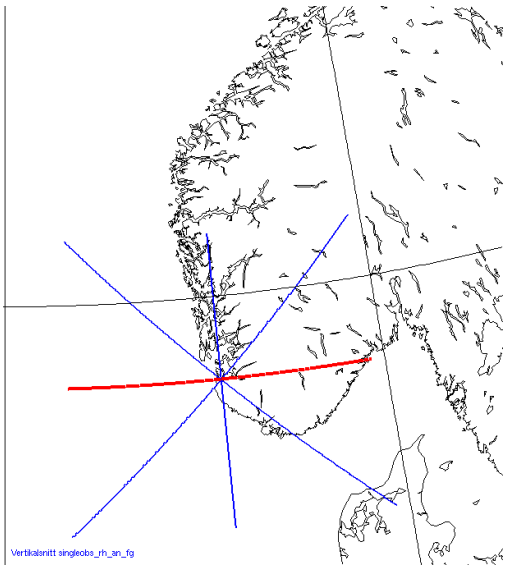

Figure 3.2: Location of the single profile of humidity observation.

Being the only observation assimilated, it is possible to compare the analysis to the models "first guess" in order to see how the assimilation process and the background error covariances performs.

3.2.1 Wind component in upper air

By extracting vertical cross-sections of "analysis minus first guess", it was discovered a problem in the increments of the V component of the wind. In Figure 3.3, this problem is shown. The vertical cross-sections correspond to the lines indicated in Figure 3.2.

There were no indication of errors on *e.g.* the wind U component. It turned out that there was a problem in the AROME code, and a fix was provided, yielding satisfactory increments when the experiment was rerun. Plots for comparison of the V component increments of the wind with and without the bug is given in Figure 3.4. This bug would probably have caused the model to drift off severely, and destroyed the entire forecast. The bugfix is implemented in all following radar data experiments.

3.2.2 Background error correlations

The background error covariance matrix $\boldsymbol{B}$ [18] plays an important role in projecting and spreading the departure (observation minus first-guess) information from the observation space to the model grids. To evaluate the accuracy of the estimated background error covariance matrix, a single observation experiment was performed.[1] Comparison of the first-guess to the analysis, in this way, shows how the single observation was taken into account – the spread was performed – during the objective analysis (3DVAR), as well as to what extend the balance between the control variables exists. This means when a humidity observation profile is assimilated, it will alter not only the humidity variables in the model, but also *e.g.* the temperature T, the wind components U, V, etc. In our example a single profile was assimilated. It turned out, that the background error statistics first used, gave far too narrow humidity increments. A new background error

[1] The experiments were run using HARMONIE 36h1.1 with the wind fix patch from Météo-France.

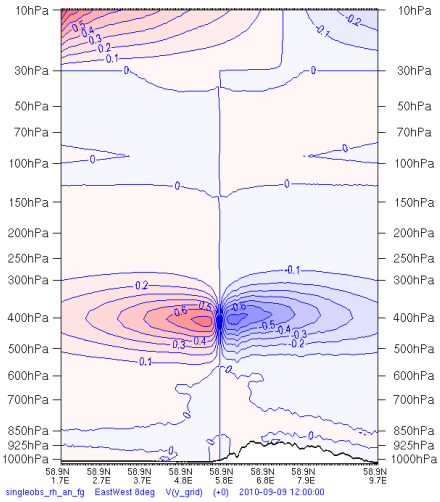

(a) East-west

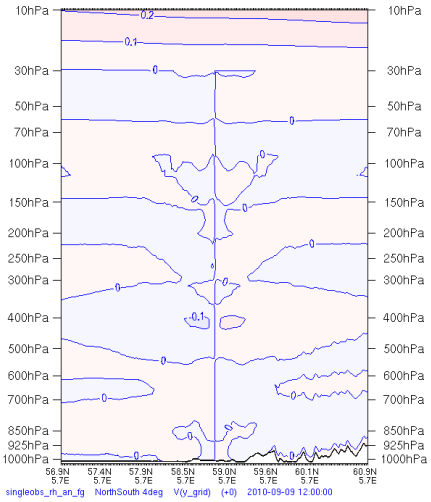

(b) North-south

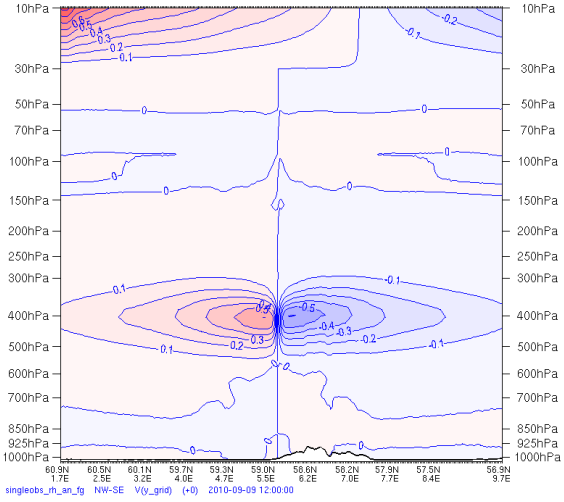

(c) NorthWest-SouthEast

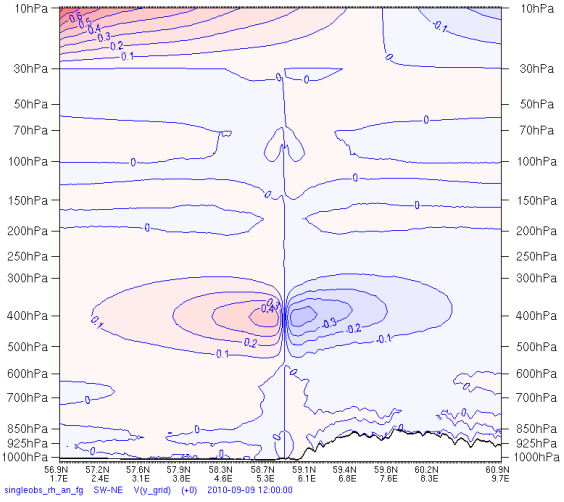

(d) SouthWest-NorthEast

Figure 3.3: Cross-sections the wind V component increments, for single profile observation of humidity. The vertical cross-sections correspond to the lines indicated in Figure 3.2. Equidistance is $1 \cdot 10^{-1}$. One can clearly see strange behavior in the stratosphere, next to the model top, 30-10 hPa.

statistics dataset was calculated, yielding better results. Figure 3.5 shows the differences. In Figure 3.5a and 3.5c, the increments are weak compared to Figure 3.5b and 3.5d (notice the different equidistance).

The narrow increments of humidity is clearly seen in BEC1 Figure 3.5a as compared to BEC2 in Figure 3.5b.

The difference between BEC1 and BEC2 is that BEC1 was estimated with lateral boundary conditions (LBCs) from a limited-area model (at 5.5 km horizontal resolution), and with lower frequency than in the BEC2. The BEC2 was computed as described in Section 2.1. So, while in BEC2 the influence of LBCs is well taken into account, in BEC1 it was almost constant along the model integration. In the case of BEC1 the influence is mostly in the analysis of small-scales (see [10] for more details). We found the BEC2 to be the most reasonable, and decided to use it in all subsequent radar assimilation experiments.

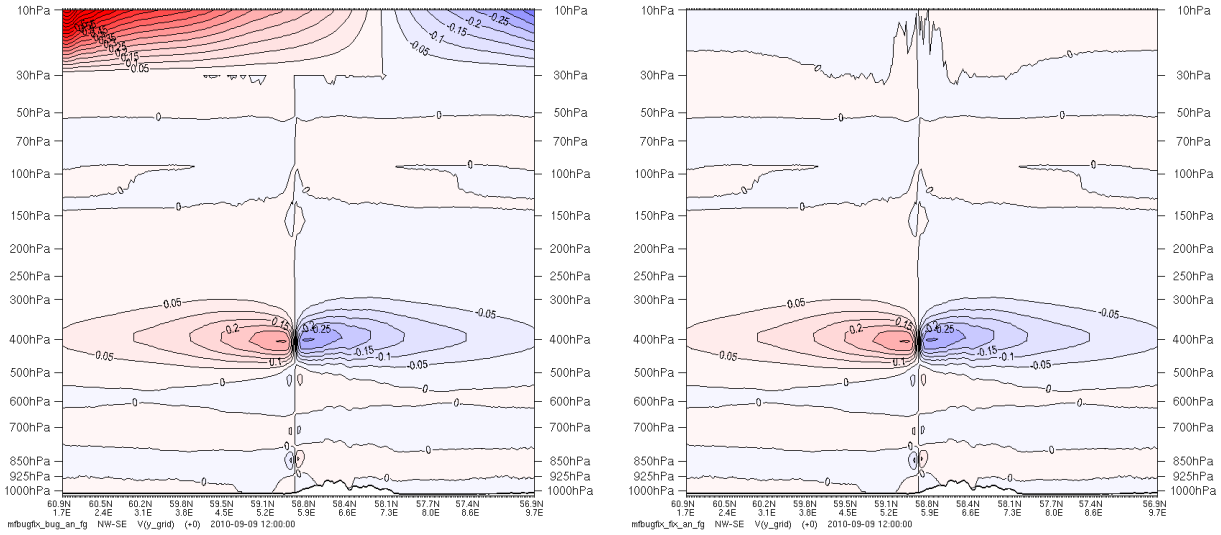

(a) With bug (NorthWest-SouthEast)

(b) With fix (NorthWest-SouthEast)

Figure 3.4: Cross-sections of the wind V component increments, from the single humidity profile experiment; **(a)** with bug, **(b)** bug fixed. Equidistance shown is $5 \cdot 10^{-2}$.

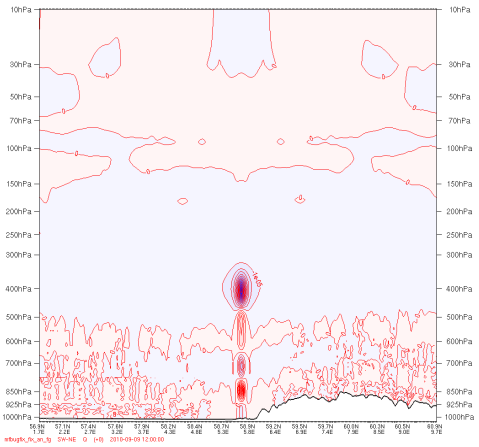

(a) BEC1: Narrow increments of humidity, Q, equidistance $1 \cdot 10^{-5}$.

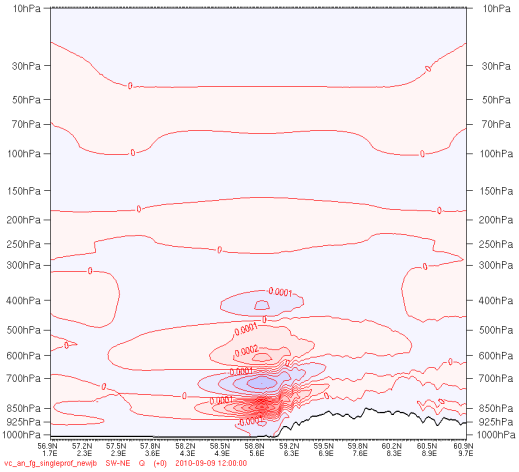

(b) BEC2: Broader and stronger increments of humidity, Q, equidistance $1 \cdot 10^{-4}$.

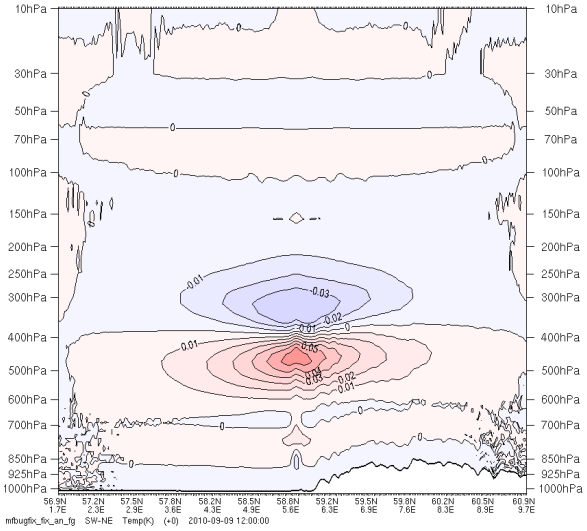

(c) BEC1: Increments in temperature, T, equidistance $1 \cdot 10^{-2}$.

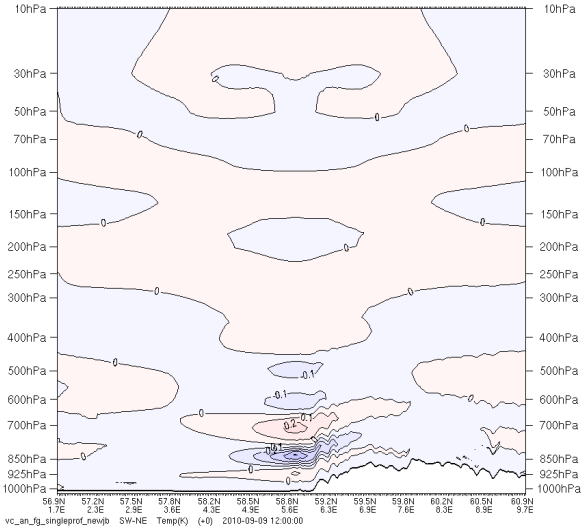

(d) BEC2: Increments in temperature, T, equidistance $1 \cdot 10^{-1}$.

Figure 3.5: Performance of the two background error covariances BEC1 and BEC2 when assimilating one single humidity profile. The vertical profiles shows the differences between the analysis and the model's first guess is plotted for **(a)** BEC1 showing narrow increments, **(b)** BEC2 showing broader and stronger increments (which is the one preferred). Corresponding plots for temperature T in **(c)** and **(d)**.

3.3 Single reflectivity observation experiment

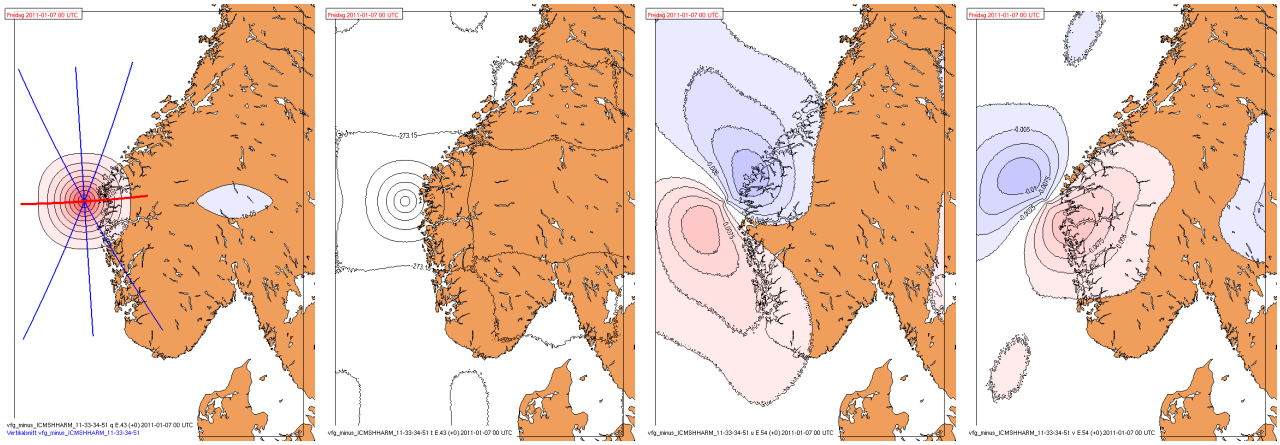

(a) Specific humidity, Q. Equidistance: $1 \cdot 10^{-5}$. **(b)** Temperature, T. Level 43. Equidistance: $1 \cdot 10^{-2}$. **(c)** Wind U component. Level 54. Equidist.: $2.5 \cdot 10^{-3}$. **(d)** Wind V component. Level 54. Equidist.: $2.5 \cdot 10^{-3}$.

Figure 3.6: Plots of model levels of the analysis increments for the single reflectivity observation.

In light of the satisfactory results on the single humidity profile and the background error statistics in Section 3.2, a new experiment was conducted with one single reflectivity observation, utilizing BEC2. Since reflectivity is converted to relative humidity before the 3DVAR assimilation step, this experiment is meant to test the performance of such a process, in conjunction with the background error statistics itself.

The results are shown in Figure 3.6 (specific humidity Q, temperature T, wind U and V component). Cross sections are shown in Figure 3.7 (specific humidity[2]), Figure 3.8 (wind U component), and Figure 3.9 (temperature T).

Both the increments and the balances with respect to wind and temperature seems acceptable.

[2]The observant reader will notice that Rudolph the red-nosed reindeer can be seen in that image.

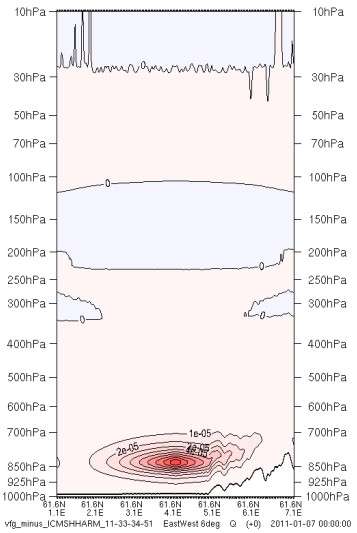

(a) East-west

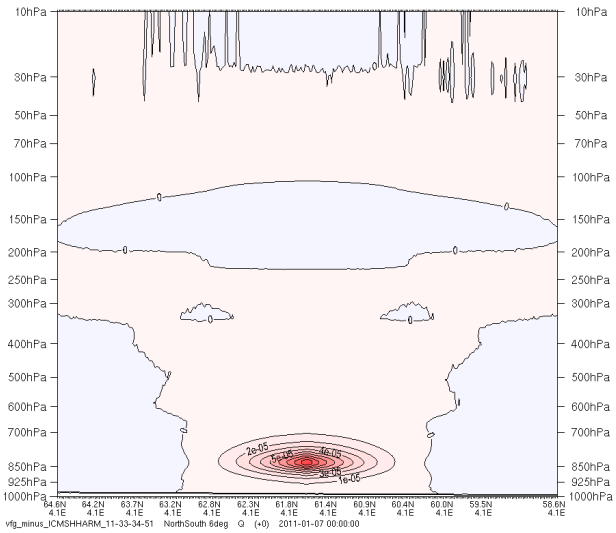

(b) North-south

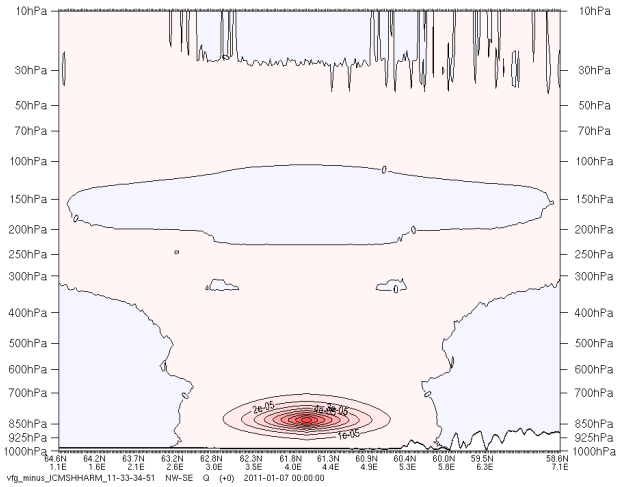

(c) NorthWest-SouthEast

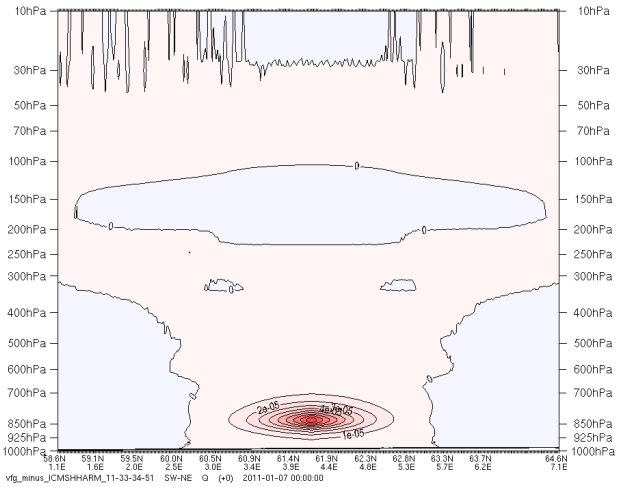

(d) SouthWest-NorthEast

Figure 3.7: Cross-sections of analysis increments on specific humidity Q for the single reflectivity observation. The vertical cross-sections correspond to the lines indicated in Figure 3.6a. Equidistance is $1 \cdot 10^{-5}$.

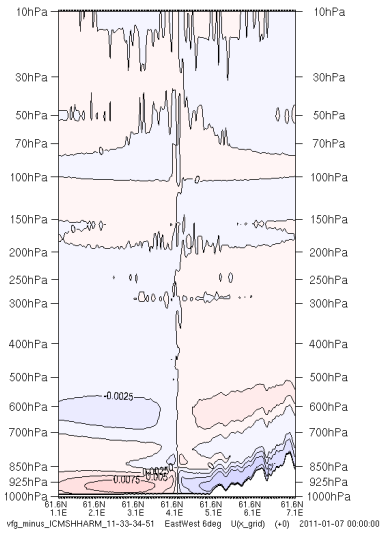

(a) East-west

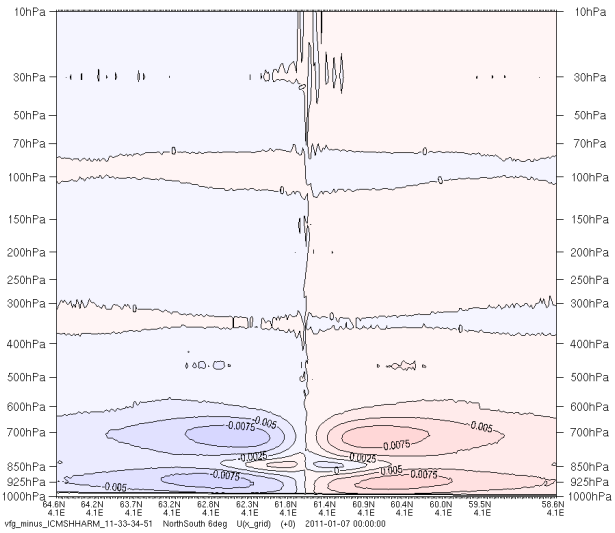

(b) North-south

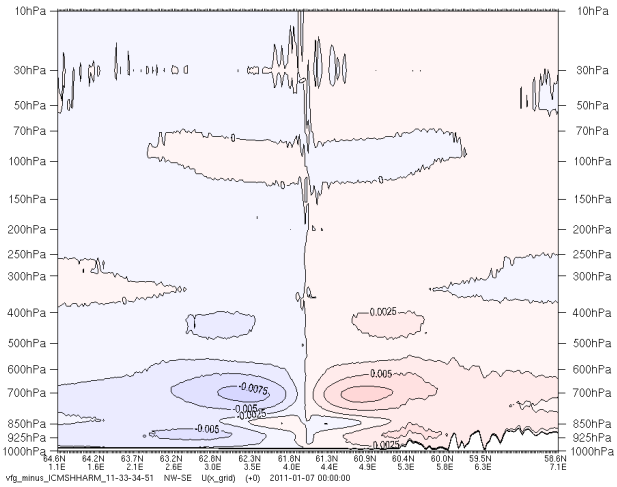

(c) NorthWest-SouthEast

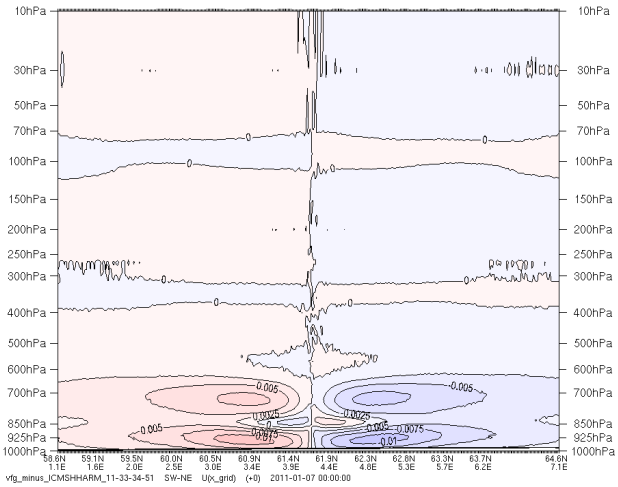

(d) SouthWest-NorthEast

Figure 3.8: Cross-sections of analysis increments on wind U component for the single reflectivity observation. The vertical cross-sections correspond to the lines indicated in Figure 3.6a. Equidistance is $1 \cdot 10^{-3}$.

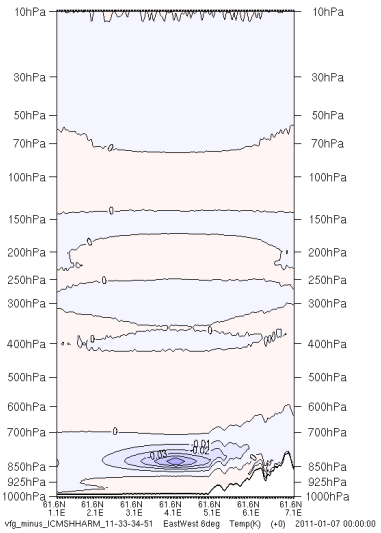

(a) East-west

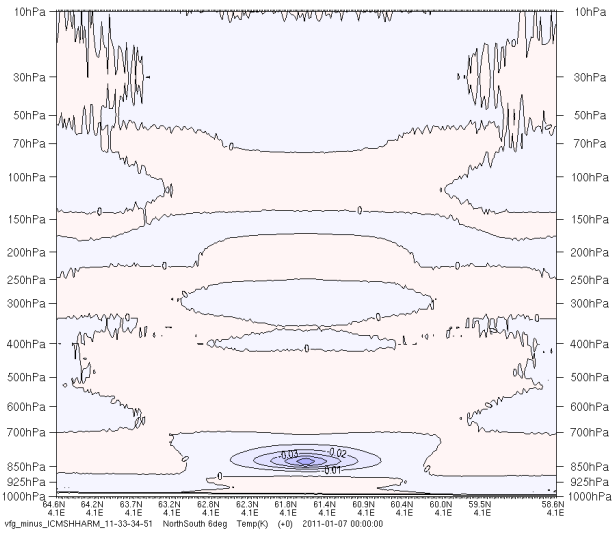

(b) North-south

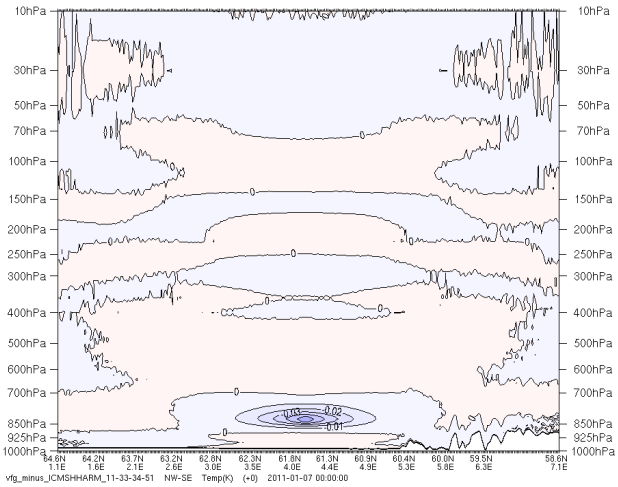

(c) NorthWest-SouthEast

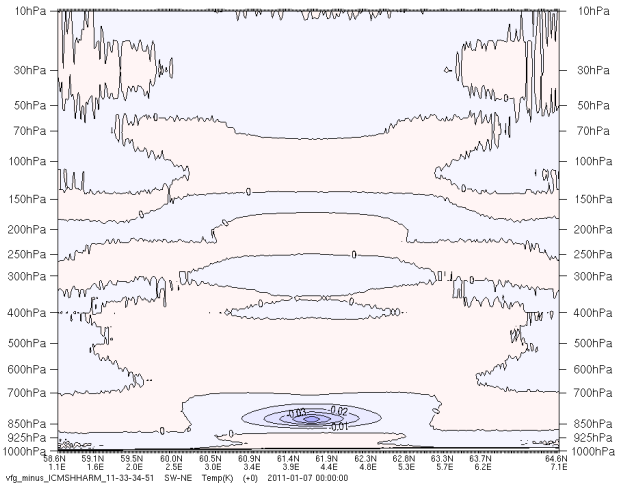

(d) SouthWest-NorthEast

Figure 3.9: Cross-sections of analysis increments on temperature T for the single reflectivity observation. The vertical cross-sections correspond to the lines indicated in Figure 3.6a. Equidistance is $1 \cdot 10^{-2}$.

3.4 Single reflectivity profile experiment

A similar experiment as that in Section 3.3 was performed, assimilating a single vertical profile of reflectivity rather than a single pixel value.

The results are shown in Figures 3.10, 3.11 and 3.12. From the plots, it can be seen that only one strong increment was achieved, as it is hard to find a profile where all data points are taken into account at the same time. So, although it looks as if a single data point was ingested, the system was given a full observation profile. The results were found to be satisfactory.

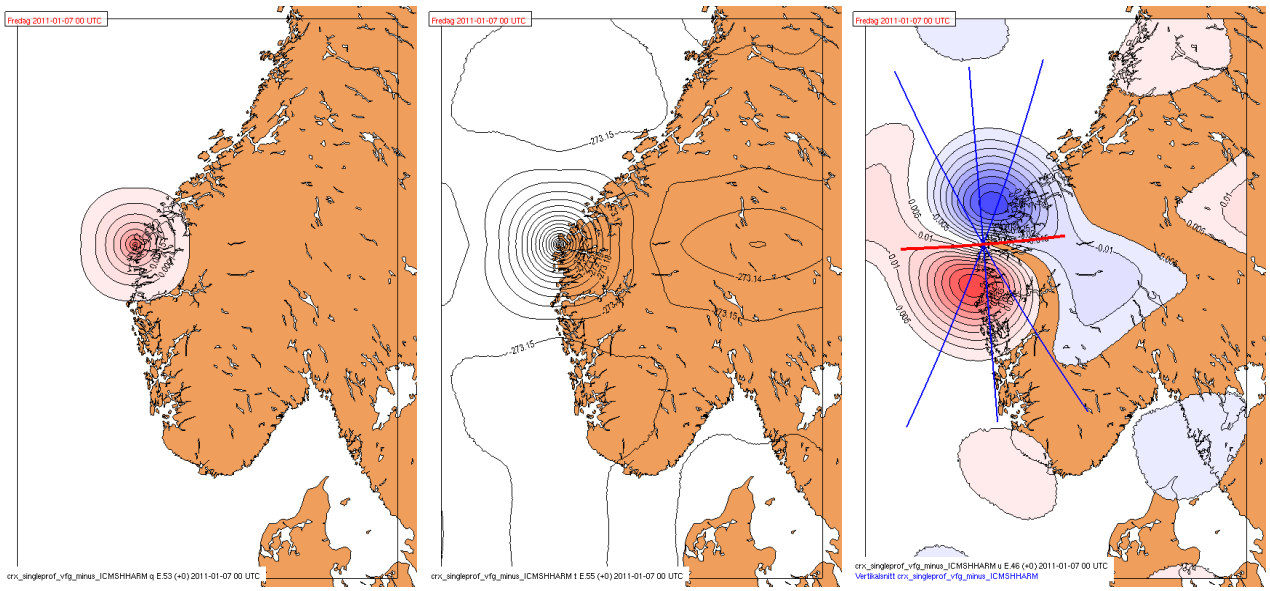

(a) Specific humidity, Q. Level 53. Equidistance: $1 \cdot 5^{-5}$.

(b) Temperature, T. Level 55. Equidistance: $1 \cdot 10^{-2}$.

(c) Wind U component. Level 46. Equidistance: $5 \cdot 10^{-3}$.

Figure 3.10: Plots of model levels of analysis increments for the single reflectivity profile experiment.

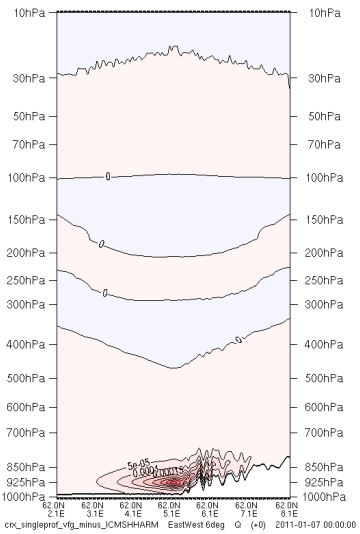

(a) East-west

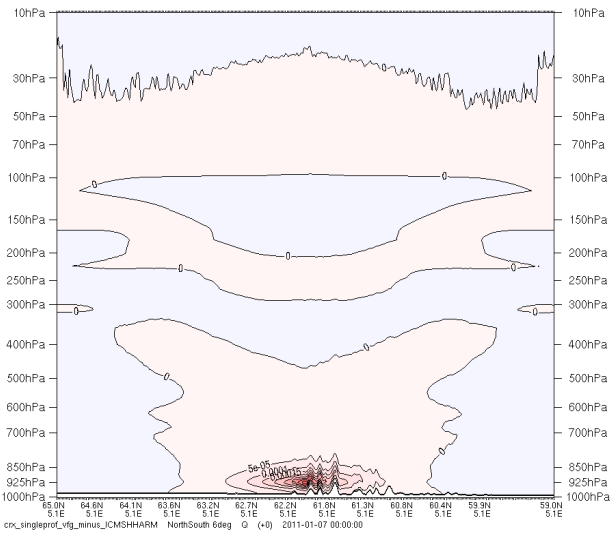

(b) North-south

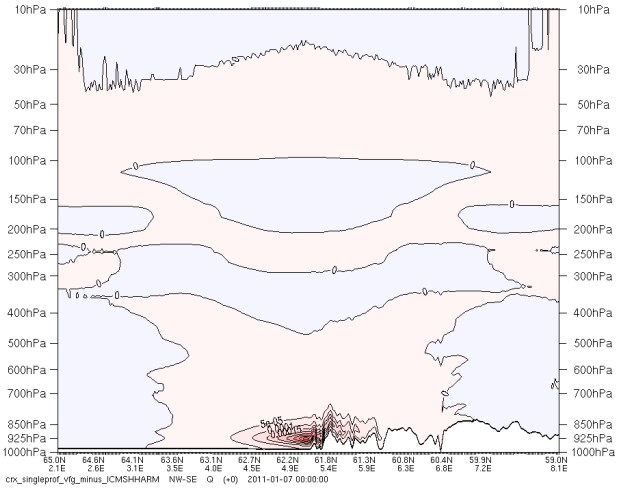

(c) NorthWest-SouthEast

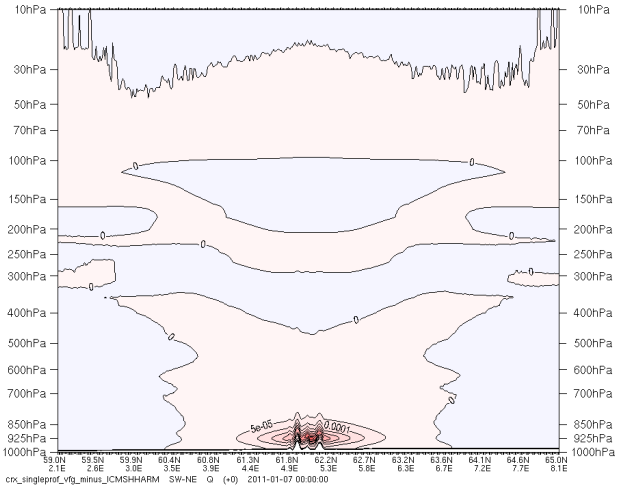

(d) SouthWest-NorthEast

Figure 3.11: Cross-sections of analysis increments on specific humidity Q for the single reflectivity profile observation. The vertical cross-sections correspond to the lines indicated in Figure 3.10c. Equidistance is $5 \cdot 10^{-5}$.

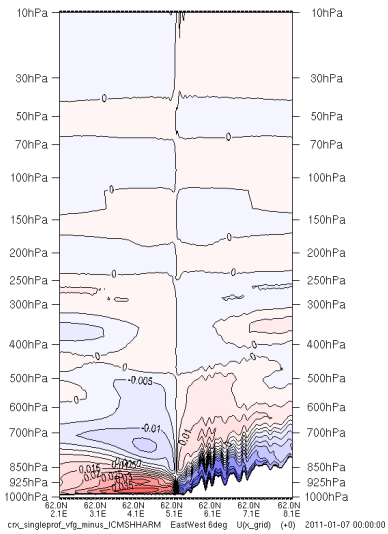

(a) East-west

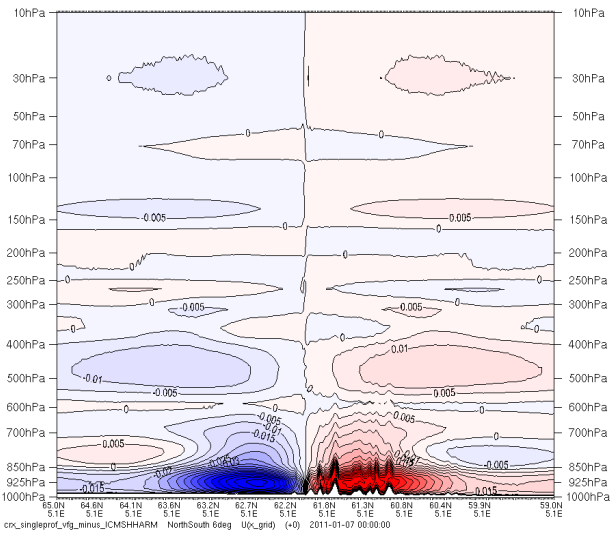

(b) North-south

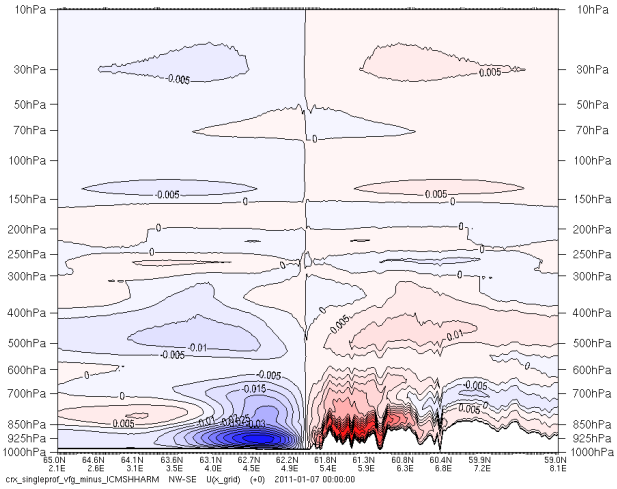

(c) NorthWest-SouthEast

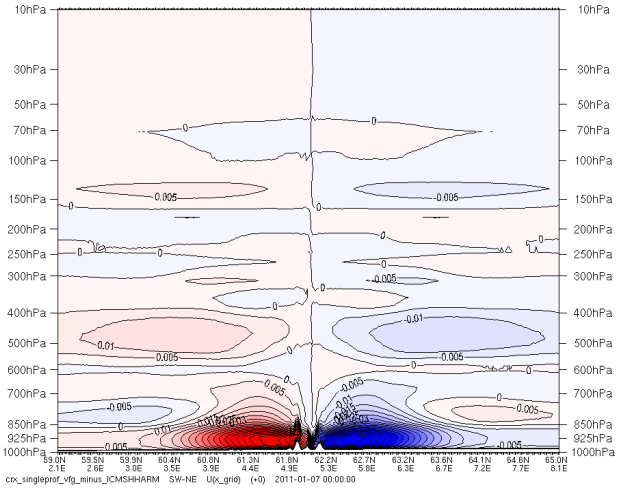

(d) SouthWest-NorthEast

Figure 3.12: Cross-sections of analysis increments on the wind U component for the single reflectivity profile observation. The vertical cross-sections correspond to the lines indicated in Figure 3.10c. Equidistance is $5 \cdot 10^{-3}$.

3.5 Evaluation of the radar reflectivity operator with 3D volume radar data

In this section, the radar simulator and inversion process is evaluated. Harmonie 36h1.4 has been used, and the experiments have been run at the ECMWF HPC facility.

3.5.1 Raw evaluation of the radar reflectivity simulator

The radar simulator, which computes simulated reflectivities based on hydrometeor contents in the model background, has been evaluated by running several tests with reflectivity assimilation. This has been done in Harmonie version 36h1.4. Figure 3.13 shows a scatter plot of observed vs. simulated reflectivity based on three cycles in a weather situation containing both dry and wet conditions. Note that this output is taken before weighting each reflectivity profile against neighboring profiles, and as such, it does not directly reflect the output of the 1D Bayesian method. Rather, this plot is meant to give a raw measure of the radar simulator. One should also note certain special values in the plot, indicated by colors:

- Blue triangles indicates values where the simulator has not found enough hydrometeors in the model background, and set the dBZ value to noise level (arbitrarily chosen to -120 dBZ).
- Orange crosses indicates values where the observed reflectivity itself has been reset to 0 dBZ. This is done to indicate lack of precipitation in both model background and observation.
- Purple plus signs indicates values where the observed and simulated reflectivities are identical. This is artificial, and as one can see, it only happens for values < 0 dBZ, which in any case indicates clear sky, *i.e.* no precipitation.

The identity line is given in gray, and so are also two vertical lines located at -10.5 dBZ (lowest possible observed value that can be represented in BATOR) and 0 dBZ (used internally to represent clear sky).

The black points show a certain increased density around the identity, but it is clear that the spread is rather large. Such plots are naturally very sensitive to the weather situation, and three cycles as shown here is not enough to draw conclusions. A more robust investigation is given in the next section.

3.5.2 Evaluation of the retrieved relative humidity

Test experiments with assimilation of radar reflectivity from five radars in the south of Norway were conducted with Harmonie 36h1.4, cycling of data at 6 h intervals, and monitoring of observation usage. Daily precipitation maps for selected days are shown in Figure 3.14.

Scatter plots of observed vs. simulated reflectivity, and pseudo-observation vs. model background of relative humidity using data from four cycles each are shown for a period with heavy rain in Figure 3.15a and 3.15b (2011-09-06, hour 00, 06, 12, 18), and less rainy in Figure 3.15c and 3.15d (2011-09-07, hour 00, 06, 12, 18).

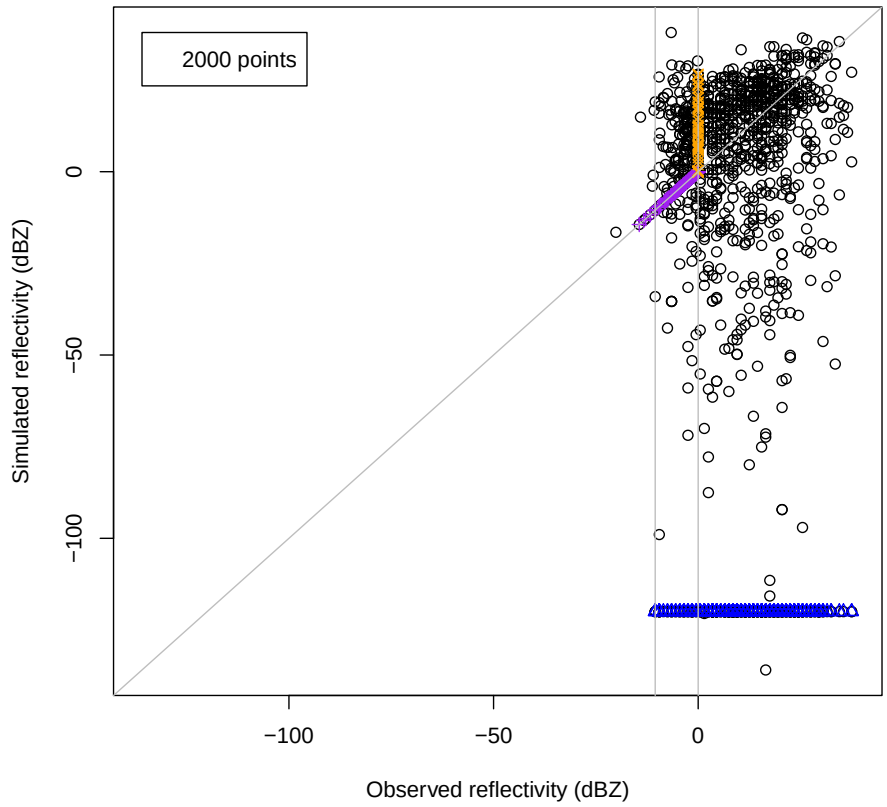

Figure 3.13: Scatter plot of observed reflectivity (dBZ) vs. simulated reflectivity (dBZ). Raw values taken before the 1D Bayesian inversion. Data from three cycles, thinned to 2000 points. See text for explanation.

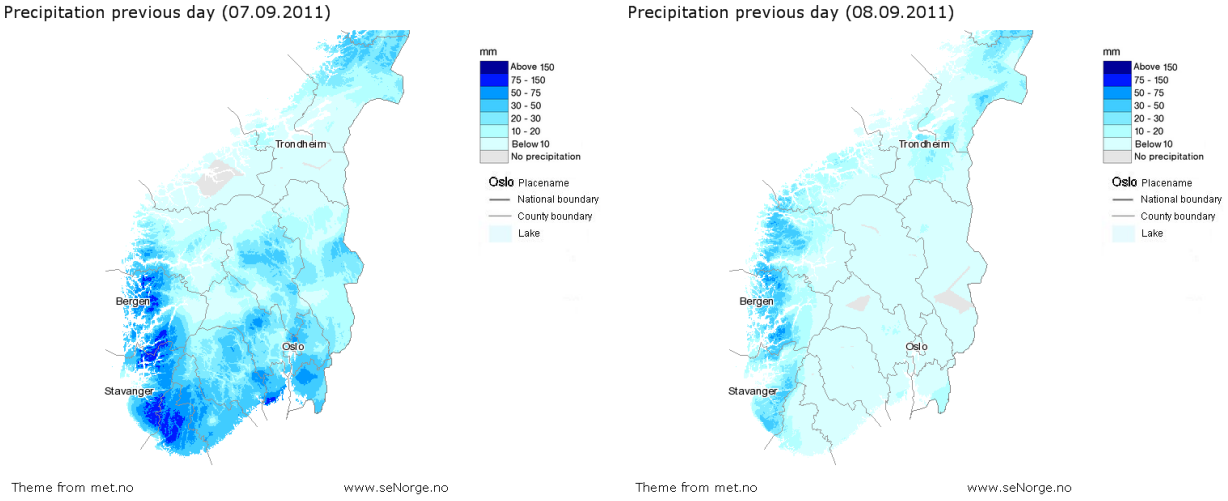

(a) Precipitation
2011-09-06 06:00 UTC – 2011-09-07 06:00 UTC

(b) Precipitation
2011-09-07 06:00 UTC – 2011-09-08 06:00 UTC

Figure 3.14: Precipitation previous day (24 hour accumulated, as of 06:00 UTC given date).

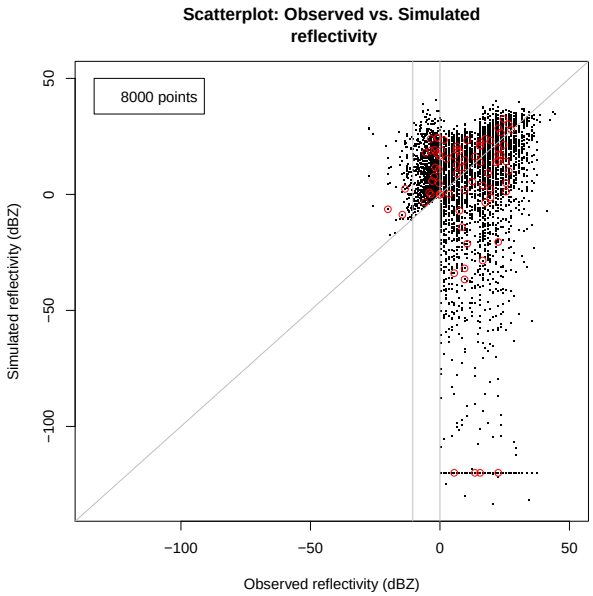

(a) 2011-09-06: Observed reflectivity (dBZ) vs. simulated reflectivity (dBZ), thinned to 8000 points.

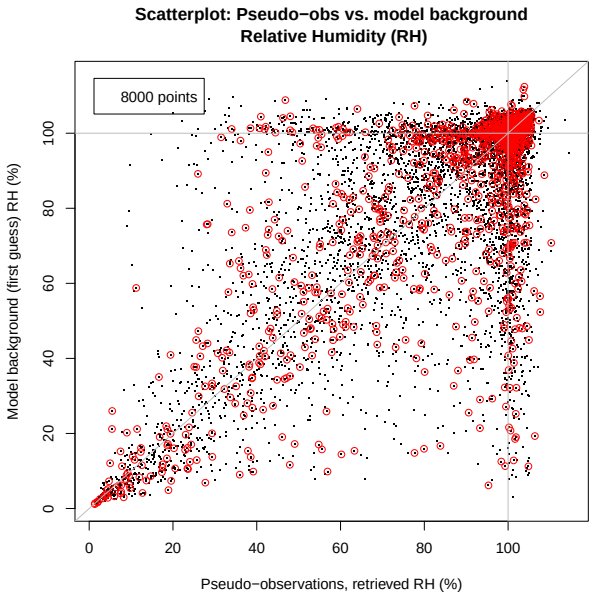

(b) 2011-09-06: Relative humidity (RH) pseudo-observations (retrieved RH) (%) vs. model background (first guess) RH (%). Thinned to 8000 points.

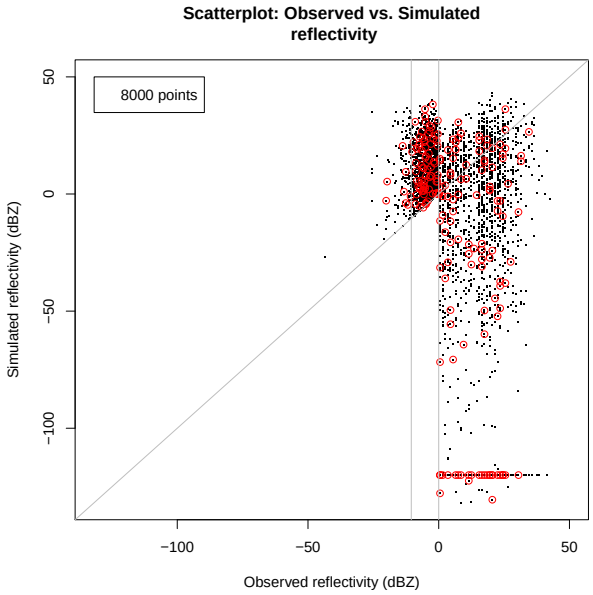

(c) 2011-09-07: Observed reflectivity (dBZ) vs. simulated reflectivity (dBZ), thinned to 8000 points.

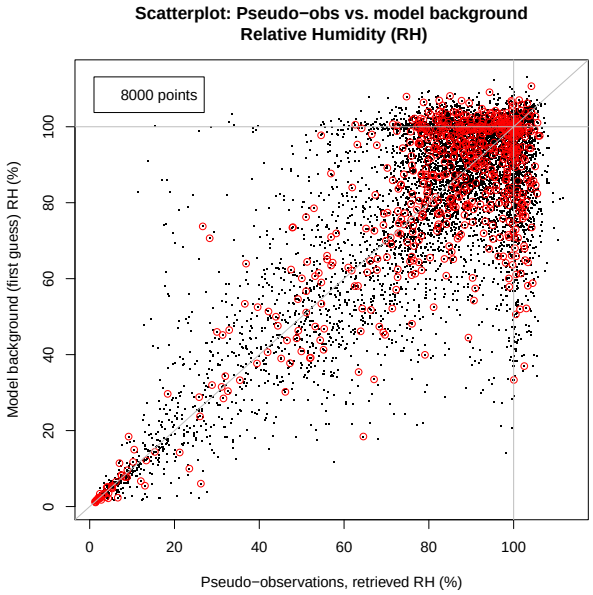

(d) 2011-09-07: Relative humidity (RH) pseudo-observations (retrieved RH) (%) vs. model background (first guess) RH (%). Thinned to 8000 points.

Figure 3.15: Scatter plot of (pseudo-)observation vs. (simulated) model background. Active values, *i.e.* after the 1D Bayesian inversion, are circled in red. Data from four cycles at 2011-09-06 (upper, heavy rain), and 2011-09-07 (lower, less rainy). See text for explanation.

3.6 Case study

This section presents a case study with assimilation of radar reflectivity data for the five southernmost radars (WMOID in parentheses): Radar Rissa (01247), Stad (01206), Bømlo (01405), Hægebostad (01438), and Hurum (01498).

All radars were quality controlled and flagged for sea-clutter, and "other-clutter". None of the radars contained flags for beam blockage.

The period considered is 2011-09-01–2011-09-09-12. Two experiments have been run in parallel, `HAR25EXP_CTRL` and `HAR25EXP_RADAR`, both cycling data at 6 h intervals with Harmonie 36h1.4, with identical configuration (boundaries from ECMWF, 3DVAR, observations; SYNOP, aircraft, buoy, TEMP(SHIP), PILOT), except for inclusion of radar reflectivity observation in one of them. See Figure 3.16b for the domain. Figure 3.17 shows the number of active humidity observations derived from radar reflectivity in the period. The weather conditions were rather dry in the domain the first day, with a precipitating system entering late September 2.

In Figure 3.16, an example of how the radar experiment is able to both dry and moist the model is shown.

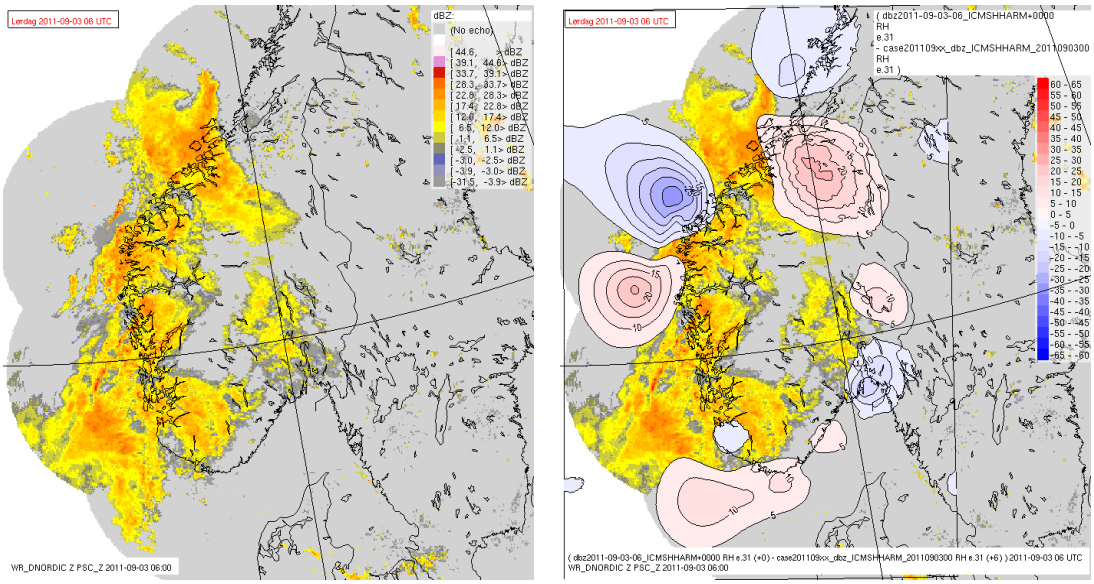

(a) Observed reflectivity at analysis time (Pseudo-CAPPI, *i.e.* reflectivity at about 500-700 m)

(b) Analysis minus first guess (model background) in relative humidity (RH) at model level 31

Figure 3.16: Analysis increments for `HAR25EXP_RADAR`. We can see that assimilation of radar reflectivity is increasing/decreasing relative humidity at appropriate places. Note that the pseudo-CAPPI plot does not reflect the full volume of observed reflectivity (which is used in the assimilation).

3.6.1 Verification scores

Figure 3.18 shows the weekly precipitation in southern Norway, last week from 2011-09-09. The verification scores compare the two models against all automatic ground stations in the domain that record hourly precipitation, pressure, temperature and wind, in total maximum 68 stations. Verification scores for hourly precipitation are given in Figure 3.19. Although only about 10 days (four assimilation times each day) are included in the statistics, we can see that assimilation of radar reflectivity observations consistently gives slightly better results. Figure 3.20 shows verification measures as a function of lead time up to six hours for pressure, temperature, wind and hourly precipitation.

A significance analysis (90 % significance level) has also been carried out, and results for surface pressure, 12 h accumulated precipitation, relative humidity and temperature are given in Figure 3.21. These are in accordance with previous plots, showing a significant (*i.e.* not at random) improvement the first hours for surface pressure, precipitation and temperature. Note that the results here go up to +48 h, whereas the pre-

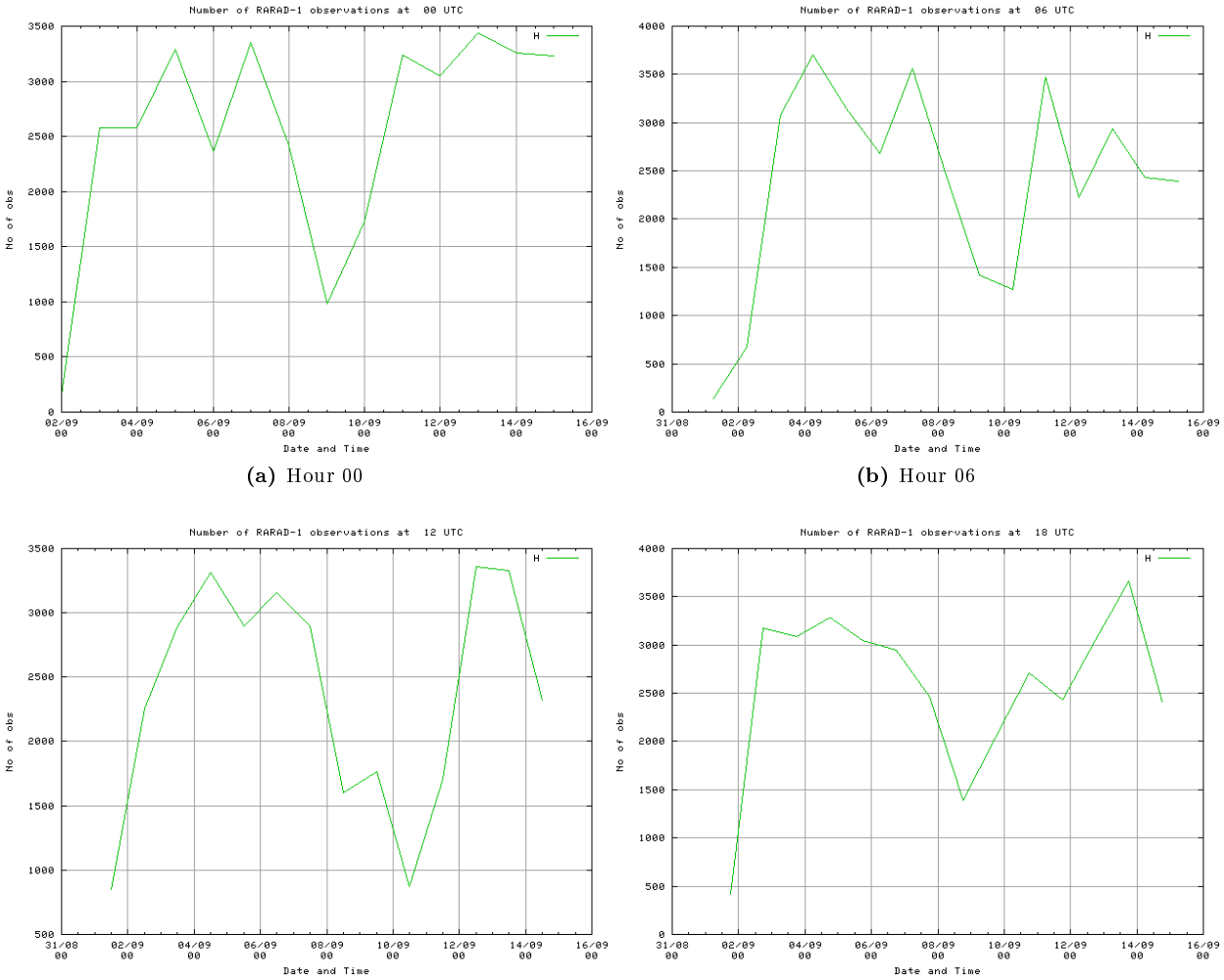

(a) Hour 00 **(b)** Hour 06

(c) Hour 12 **(d)** Hour 18

Figure 3.17: Active humidity observations derived from radar reflectivity data. The domain is given in Figure 3.16b.

vious figures in the section only go to +6 h. The values are given as `HAR25EXP_CTRL` minus `HAR25EXP_RADAR`, so positive values are in favor of the experiment with radar data assimilation. For *e.g.* precipitation, we can see a positive impact until +36 hours. This is near the predictability limit, and one should also take into account that the model domain is rather small (see Figure 3.16b). A larger domain, and a longer time series, could potentially improve these scores.

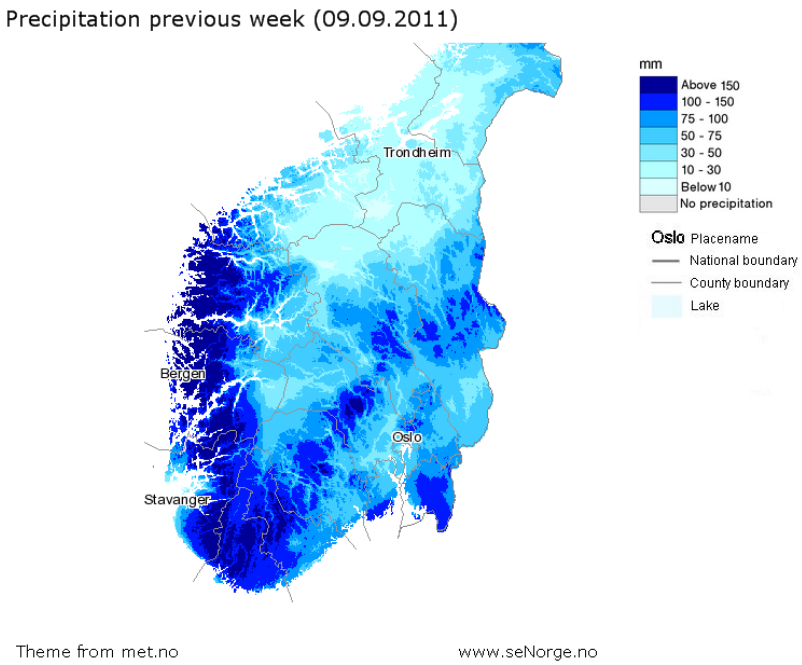

Figure 3.18: Weekly precipitation in southern Norway, previous week from 2011-09-09.

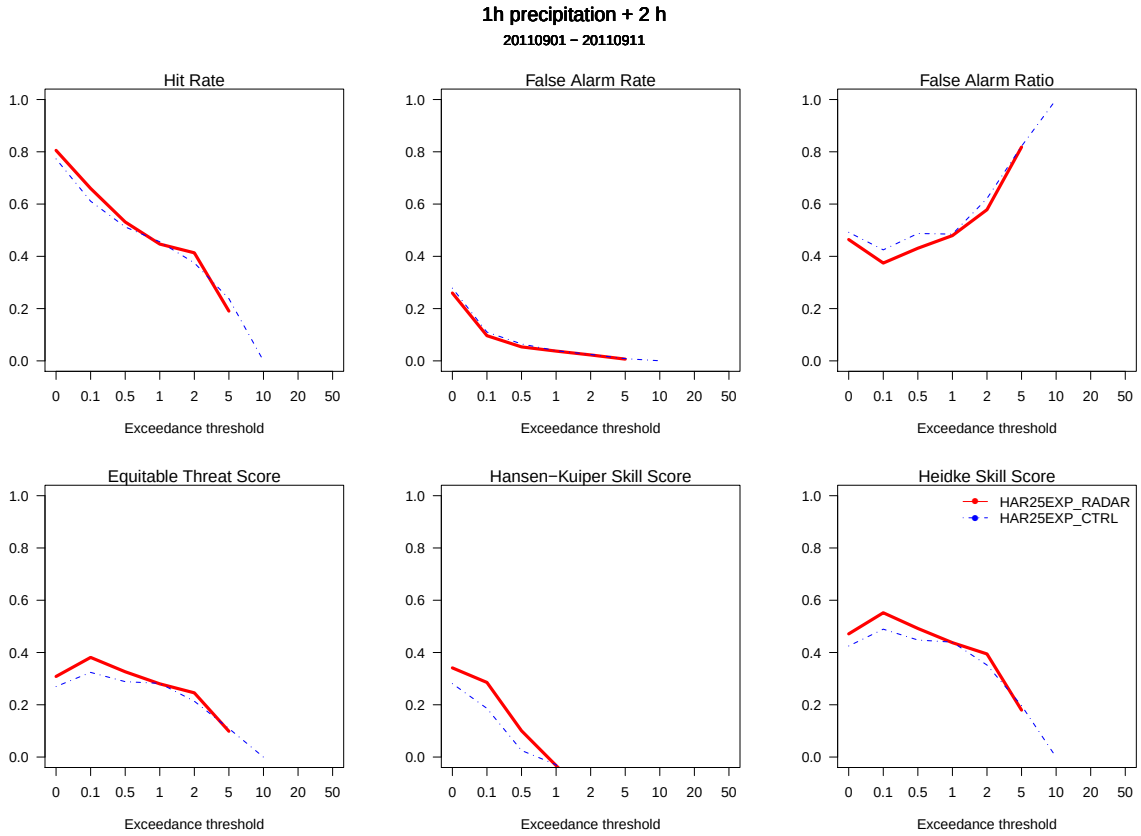

(a) Lead time +2 h

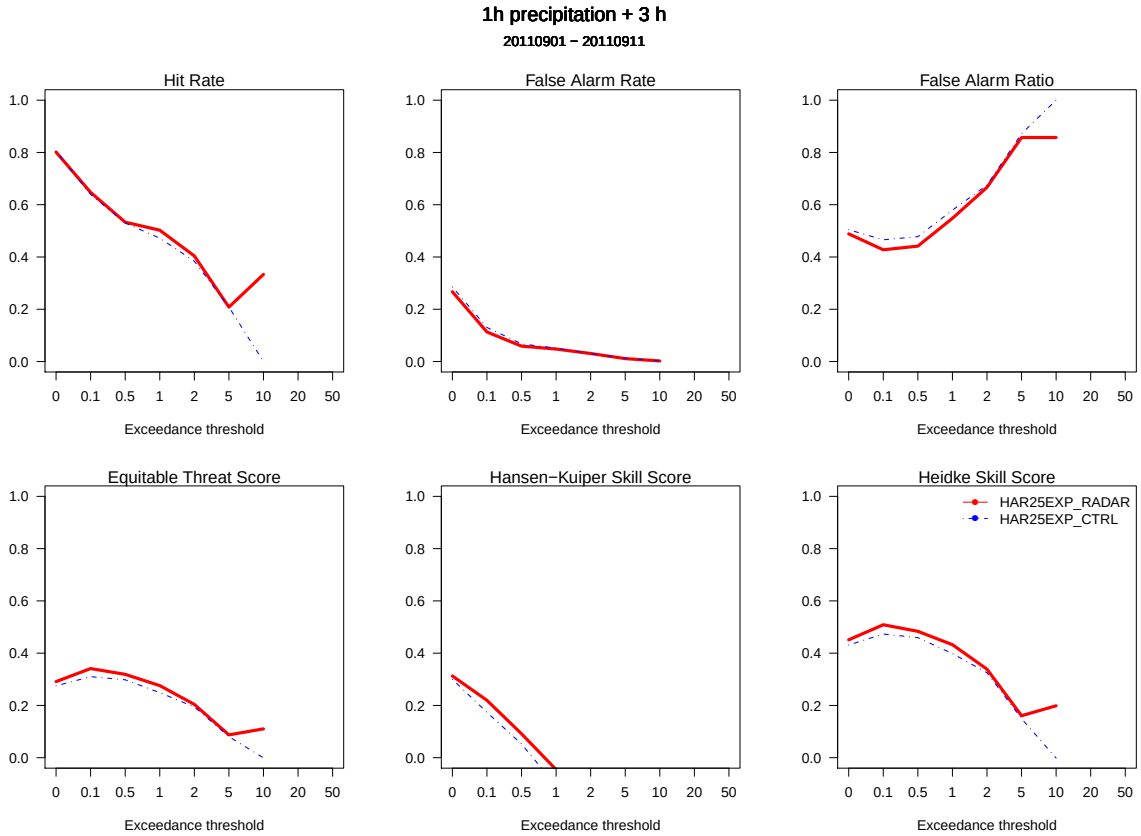

(b) Lead time +3 h

Figure 3.19: Scores for 1 h accumulated precipitation for different lead times. In the lower panels scores which summarize the upper panels are shown. Higher score is better, which shows consistently better results for the radar experiment (line in red) than the control experiment (thin dash-dotted line in blue). (Continued)

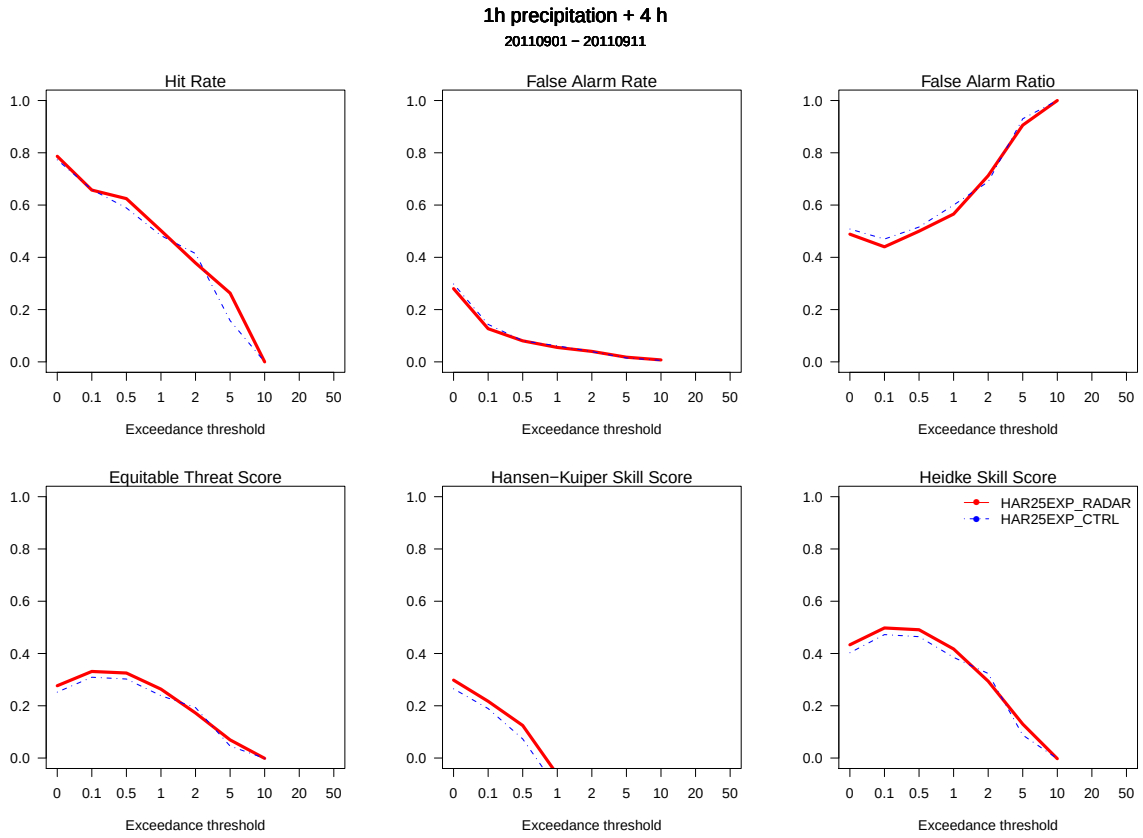

(c) Lead time +4 h

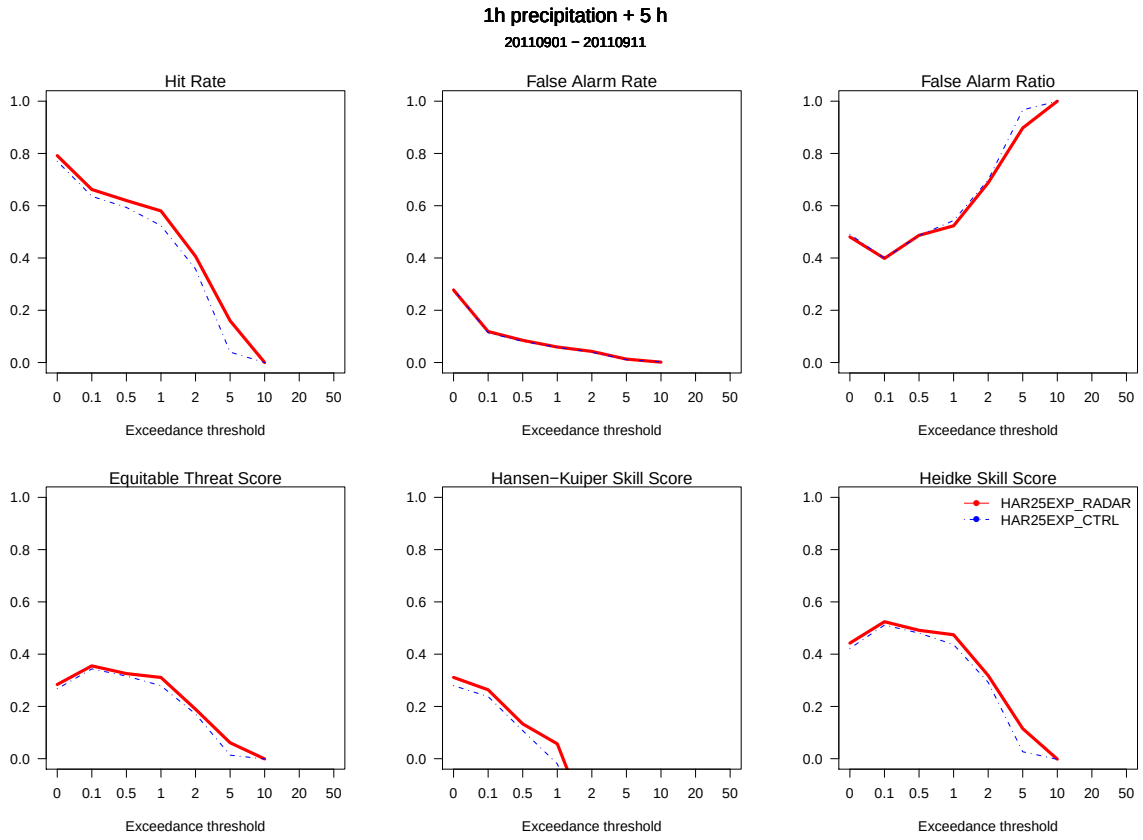

(d) Lead time +5 h

Figure 3.19: (Continued:) Scores for 1 h accumulated precipitation.

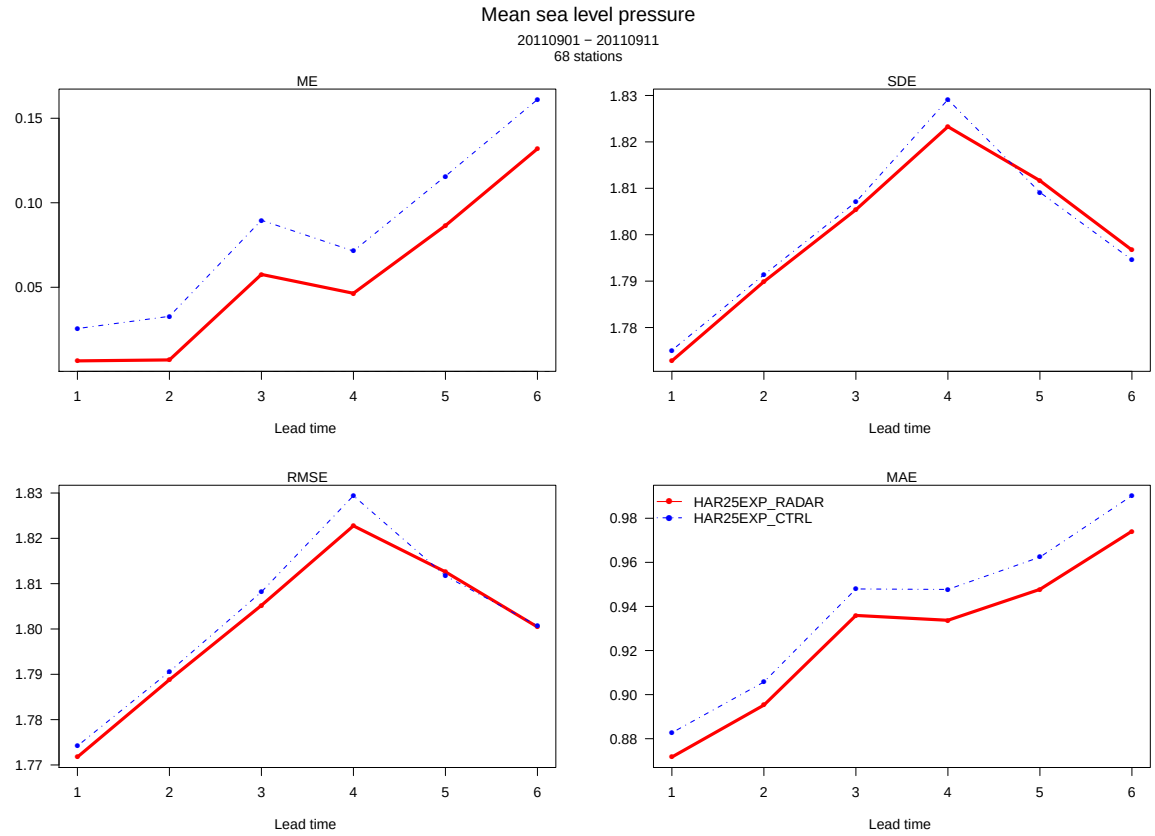

(a) Mean sea level pressure (MSLP)

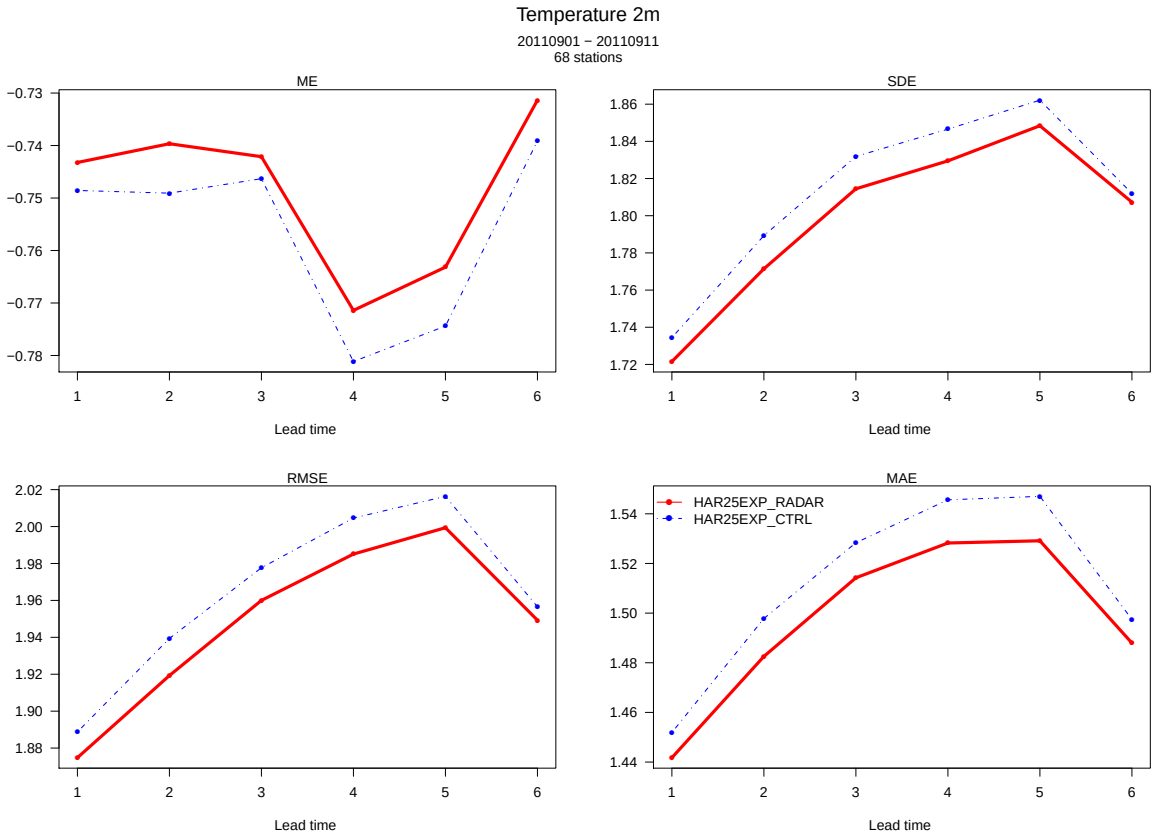

(b) 2 m temperature

Figure 3.20: Mean Error (ME), Standard Deviation Error (SDE), Root Mean Square Error (RMSE), and Mean Absolute Error (MAE) for the given parameters. The radar experiment is given in red, and the control experiment in thin dash-dotted blue line. The results are better when the values are approaching zero. (Continued.)

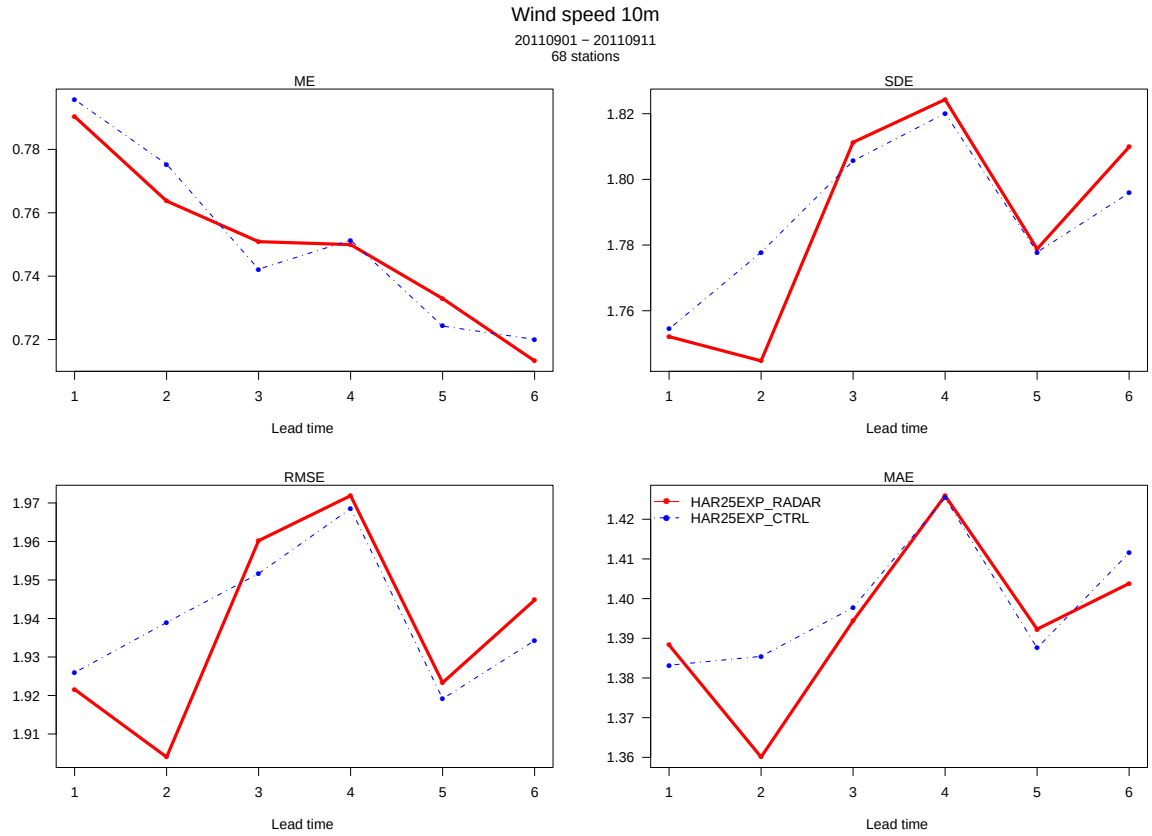

(c) 10 m wind

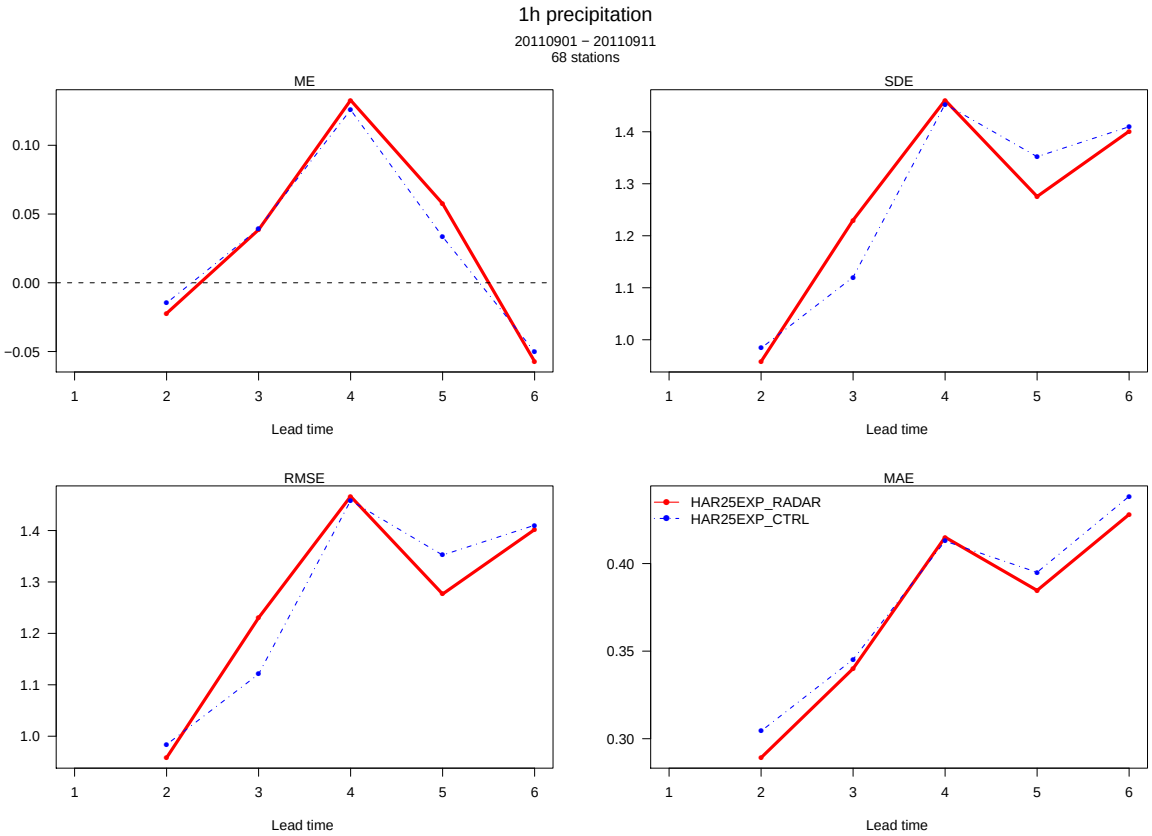

(d) 1 h accumulated precipitation

Figure 3.20: (Continued:) Mean Error (ME), Standard Deviation Error (SDE), Root Mean Square Error (RMSE), and Mean Absolute Error (MAE) for the given parameters. The radar experiment is given in red, and the control experiment in thin dash-dotted blue line. The results are better when the values are approaching zero.

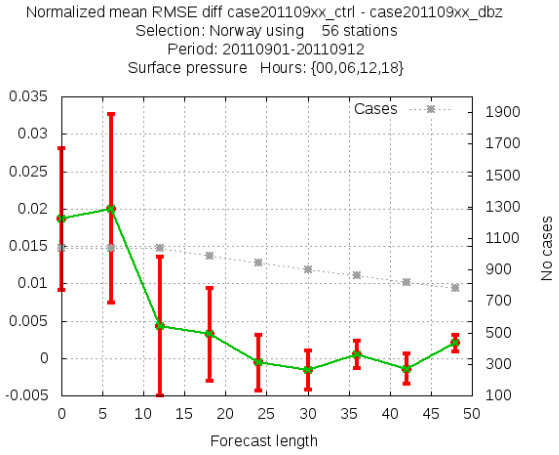

(a) Surface pressure (PS)

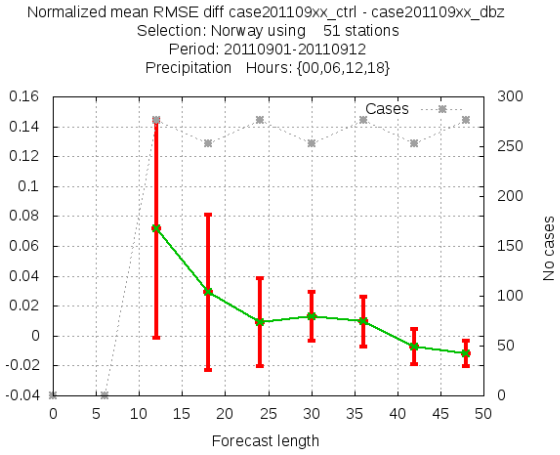

(b) Precipitation (12 h accumulated)

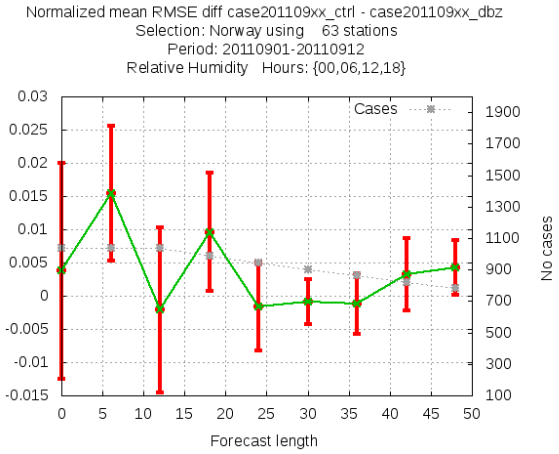

(c) Relative humidity (RH)

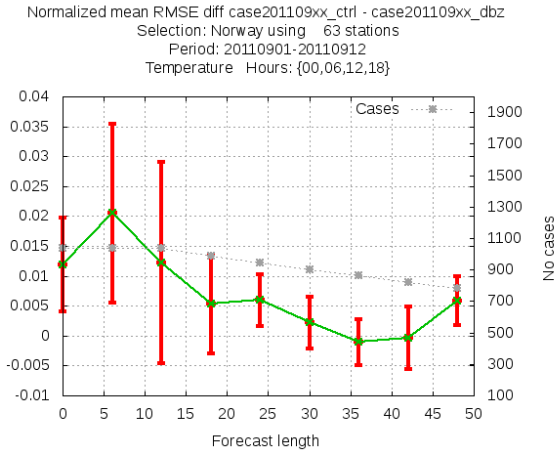

(d) Temperature

Figure 3.21: Normalized difference in RMSE in given parameters. Note that this is CTRL minus RADAR, so positive numbers are in favor of radar assimilation. Period 2011-09-01–2011-09-12, forecast length +48 h. Significance level 90 %.

Chapter 4

Concluding remarks

We have demonstrated a fully functional conversion tool, CONRAD, that successfully transfers Norwegian radar observations all the way from the local format, via Météo-France BUFR, BATOR, ODB and to the assimilation system in HARMONIE.

The model response to such observations has been carefully investigated in terms of single (profile) observation experiments. A problem in the AROME code was discovered and patched, and it was settled for a satisfactory background error statistics dataset.

Verifying the model performance with radar reflectivity against the surface observations lead to the following statements i) from the assimilation point of view, radar reflectivity improves significantly the forecast up to six hours, *i.e.* produces better first guess for the assimilation system, ii) in overall, radar reflectivity improves the forecast up to 12-36 hours depending on the verified parameter. For example 2 m temperature is improved until +30 h, precipitation improves the forecast until +36 h and surface pressure until +18 hours.

It should be noted that the experiments were run for a relatively short period and in a relatively small domain, which affects the impact on longer lead times, as shown in the results.

Although in the specific cases presented, which demonstrated that the system is able to moisten and dry the analysis consistently, it would be of interest to extend the test period and investigate a heterogeneous background error statistics [19], where dry and moist air are considered separately.

Bibliography

[1] G. Bölöni, Overview of radar data assimilation in NWP models, http://www.rclace.eu/?page=11, 2008.

[2] P. Meischner, *Weather radar: principles and advanced applications*, Physics of earth and space environments, Springer, 2004.

[3] T. Montmerle et al., Regional scale assimilation of radar data at Météo-France, HIRLAM Technical Report 68, Météo-France, 2008.

[4] E. Wattrelot, O. Caumont, S. Pradier-Vabre, M. Jurasek, and G. Haase, 1D+3Dvar assimilation of radar reflectivities in the pre-operational AROME model at Météo-France, in *ERAD2008*, 2008, http://erad2008.fmi.fi/proceedings/extended/erad2008-0097-extended.pdf.

[5] O. Caumont, V. Ducrocq, G. Jaubert, and S. Pradier-Vabre, Tellus A **62**, 173 (2010), doi:10.1111/j.1600-0870.2009.00430.x, [link].

[6] C. A. Elo, Correcting and quantifying radar data, met.no report 2/2012 ISSN 1503-8025, met.no, 2012, http://met.no/Forskning/Publikasjoner/.

[7] M. Salomonsen, PRORAD, https://wiki.met.no/prorad/.

[8] Y. Seity et al., Mon. Wea. Rev. **139**, 976 (2010), doi:10.1175/2010MWR3425.1, [link].

[9] L. Isaksen, M. Fisher, and J. Berner, Use of analysis ensembles in estimating flow-dependent background error variance, 2007, paper presented at Workshop on Flow-Dependent Aspects of Data Assimilation http://www.ecmwf.int/publications/library/do/references/list/14092007.

[10] A. Storto and R. Randriamampianina, J. Geophys. Res. **115** (2010), doi:10.1029/2009JD013111, [link].

[11] L. Berre, Mon. Wea. Rev. **128**, 644 (2000), doi:10.1175/1520-0493(2000)128<0644:EOSAMF>2.0.CO;2, [link].

[12] F. Bouttier, Arome system documentation, Technical report, CNRM/GAME, Météo-France, 2009.

[13] O. Caumont et al., J. Atmos. Oceanic Technol. **23**, 1049 (2006), [link].

[14] M. S. Grønsleth and C. A. Elo, NOTUR II META **4**, 17 (2011), ISSN: 1890-2987, [link].

[15] M. S. Grønsleth, CONRAD presentation, 2012, https://svn.hirlam.org/branches/harmonie-36h1_radar/util/conrad/doc/conrad-pres.pdf (restricted access).

[16] M. S. Grønsleth, CONRAD reference manual, 2012, https://svn.hirlam.org/branches/harmonie-36h1_radar/util/conrad/doc/conrad-refman.pdf (restricted access).

[17] M. S. Grønsleth and F. T. Tveter, Preprocessing and "1D-VAR" simplified assimilation system for radar reflectivity, 2010, http://met.no/Forskning/Publikasjoner/?module=Files;action=File.getFile;ID=3342.

[18] A. C. Lorenc, Quarterly Journal of the Royal Meteorological Society **112**, 1177–1194 (1986), doi:10.1002/qj.49711247414, [link].

[19] T. Montmerle and L. Berre, Quarterly Journal of the Royal Meteorological Society **136**, 1408 (2010), doi:10.1002/qj.655, [link].

Glossary

1DVAR One dimensional variational (data assimilation). 4

3DVAR Three dimensional variational (data assimilation). 1, 3, 4, 8, 22

AEMET Spanish State Meteorological Agency. 3

ALADIN The community using and developing the ALADIN NWP framework. i, 3

ALADIN "Aire Limitée, Adaptation dynamique, Développement INternational" (Limited Area, Dynamic Adaptation, International Development) – A limited area-version of ARPEGE/IFS. 35

AROME "Application of Research to Operations at MesoscalE". A non-hydrostatic meso-scale NWP model with a sophisticated physical parameterization package. Started in 2000 at Météo-France. 1, 3, 4, 8, a, 31

BATOR A tool for feeding the ODB with observations read from (BUFR) files. Part of HARMONIE. 4–7, 19, 31

BUFR "Binary Universal Form for Representation of meteorological data". A binary data format maintained by WMO. i, 5, 7, 31, 35

CAPPI Constant Altitude Plan Position Indicator (Constant Altitude PPI). A radar display which gives a horizontal cross-section of data at constant altitude. 36

CONRAD CONversion of RAdar Data. A tool for converting *e.g.* PRORAD XML to BUFR. 5, 7, 31

dBZ Decibels of Z; a meteorological measure of equivalent reflectivity (Z) of a radar signal reflected off a remote object. 3

DMI Danish Meteorological Institute. 3

ECMWF The European Centre for Medium-Range Weather Forecasts (ECMWF). An intergovernmental organization supported by 34 states, based in Reading, UK. i, 19, 22

EMHI Estonian Meteorological Institute. 3

FMI Finnish Meteorological Institute. 3

HARMONIE "HIRLAM ALADIN Regional Meso-scale Operational NWP In Europe". The next generation NWP system developed by the HIRLAM consortium. i, 1, 3–5, 7, 8, a, 31, 35, 36

HIRLAM The community using and developing the NWP framework HIRLAM and HARMONIE. i, 3, 35

HIRLAM "HIgh Resolution Limited Area Model", a NWP system used by the HIRLAM community. 3, 35

HPC High-performance computing: Supercomputers or computer clusters. 3, 19

KNMI Royal Netherlands Meteorological Institute. 3

LAM Local Area Model. 1

LBC Lateral Boundary Condition. 9

LHMS Lithuanian Hydrometeorological Service. 3

Météo-France French national meteorological service. 3

Met Eireann Irish Meteorological Service. 3

met.no The Norwegian Meteorological Institute. 3, 4

NWP Numerical Weather Prediction. 1, 3, 4, 6, 35

ODB Observational DataBase: Database holding all observations in the HARMONIE system. Can mimic relational database queries through its ODB/SQL-compiler. 5, 7, 31

OMSZ The Hungarian Meteorological Service. i

PCAPPI Pseudo Constant Altitude Plan Position Indicator (Pseudo-CAPPI). An extended CAPPI, where the lowest elevation is used to fill in data at long distances, and highest elevation is used to fill in data close to the radar site. 5

PPI Plan Position Indicator. A 2D display of the airspace around a radar site for a given elevation. 5, 6, 35

PRORAD PROduction system for RADar data. 4

PRORAD XML File format used by PRORAD. Supports cartesian and polar PPI, and polar volume data.. 4, 5, 7, 35

SMHI Swedish meteorological and Hydrological Institute. 3

SYNOP Surface synoptic observations. 3

VI Icelandic Meteorological Office. 3

WMO World Meteorological Organization. 35

XML EXtensible Markup Language. 4